Aus der Klinik für Nephrologie
der Medizinischen Fakultät Charité – Universitätsmedizin Berlin

DISSERTATION

Signaling Pathway for Serum Amyloid A Mediating Inflammatory Reactions in Macrophages

zur Erlangung des akademischen Grades
Doctor medicinae (Dr. med.)

vorgelegt der Medizinischen Fakultät
Charité – Universitätsmedizin Berlin

von

Hu, Xiu-Ping

aus Lishui, Zhejiang, China

Datum der Promotion: 4. Juni 2021

Preface

The dissertation was developed during my work in the lab of Nephrology of the Charité - Universitätsmedizin Berlin from December 2016 to June 2019. The experimental research was funded by the Charité, the Sonnenfeld Stiftung and Fokus Area Dynage.

Part of the experimental results have been published as abstract and poster presentation at the annual congress in 2018 of the “Deutsche Gesellschaft für Nephrologie” at Berlin. Furthermore, part of the results from this research has been published in “Schuchardt M, Prufer N, Tu Y, Herrmann J, Hu XP, Chebli S, Dahlke K, Zidek W, van der Giet M, Tolle M. 2019. Dysfunctional high-density lipoprotein activates toll-like receptors via serum amyloid A in vascular smooth muscle cells. Sci Rep 9: 3421”(doi 1038/s41598-019-39846-3).

Contents

Tables

Figures

List of abbreviations

Abbreviation	Meaning
apoA-Ⅰ	Apolipoprotein A Ⅰ
ARDS	Acute respiratory distress syndrome
A-SAA	Acute serum amyloid A
ATP	Adenosine triphosphate
ATF5	Activating transcription factor
BCA	Bicinchoninic acid
CBP	Cardiopulmonary bypass
CD	Cluster of differentiation
cDNA	Complementary DNA
CHE	Cholesterol esterase
CHO	Cholesterol oxidase
CK-1	Casein kinase 1
CKD	Chronic kidney disease
CNS	Central nervous system
CRP	C-reactive protein
CO_2	Carbon dioxide
C-SAA	Constant serum amyloid A
CVD	Cardiovascular disease
CXCL 1	Chemokine (C-X-C motif) ligand 1
DAMPs	Damage-associated molecular patterns
DHE	Dihydroethidium
DKD	Diabetic kidney disease
DMEM	Dulbeccos's modified eagle medium
DMSO	Dimethyl sulfoxide
DPI	Diphenyliodonium
EDTA	Ethylenediaminetetraacetic acid
ELISA	Enzyme-linked immunosorbent assay
ERK	Extracellular signal–regulated kinases
FBS	Fetal bovine serum
FPR2	Formyl peptide receptor 2
GAGs	Glycosaminoglycans
GAPDH	Glyceraldehyde-3-Phosphate Dehydrogenase
G-CSF	Granulocyte colony-stimulating factor
GK	Glycerol kinase
GM-CSF	Granulocyte-macrophage colony-stimulating factor
GPO	Glycerol-3-phosphate-oxid
HCO	High-molecular weight cut-off
HD	Hemodialysis
HDF	Hemodiafitration

Abbreviation	Meaning
HDL	High-density lipoprotein
HF	Hemofiltration
HMGB1	High mobility group box 1
HVHF	High-volume hemofiltration
ICAM-1	Intercellular adhesion molecule 1
IκBα	Nuclear factor of kappa light polypeptide gene enhancer in B-cells inhibitor, alpha
IL	Interleukin
IRF-7	Interferon regulatory factor 7
c-JNK	c-Jun N-terminal kinases
LDL	Low-density lipoprotein
oxLDL	Oxidized low density lipoprotein
LPL	Lipoprotein lipase
LPS	Lipopolysaccharide
MAPK	Mitogen-activated protein kinase
MCP-1	Monocyte chemoattractant protein 1
MMP	Matrix metalloproteinase
mRNA	Messenger RNA
MyD88	Myeloid differentiation primary response 88
NADPH	Nicotinamide adenine dinucleotide phosphate
NED	N-1-napthylethylenediamine dihydrochloride
NF-κB	Nuclear factor kappa-light-chain-enhancer of activated B cells
NLRP3	NOD-like receptor family, pyrin domain containing 3
NO	Nitric oxide
NOS	NO synthase
eNOS	Endothelial NOS
iNOS	Inducible NOS
nNOS	Neuronal NOS
NOX2	NADPH oxidase 2
PAMPs	Pathogen-associated molecular patterns
PBMC	Peripheral blood mononuclear cell
PBS	Phosphate-buffered saline
PDO	4-aminoantipyrine peroxidase
PMA	Phorbol 12-myristate 13-acetate
$P2X_7$	P2X purinoceptor 7
RAGE	Receptor for advanced glycation endproducts
ROS	Reactive oxygen species
RPMI	Roswell Park Memorial Institute
SAA	Serum amyloid A

Zusammenfassung

Das inflammatorische Milieu bei Patienten mit einer chronischer Nierenerkrankung (CNI) ist ein Risikofaktor für vaskuläre Komorbiditäten. Bislang sind verschiedene Biomarker hierfür bei CNI Patienten identifiziert, einer davon ist das Serumamyloid A (SAA). SAA ist ein Akut-Phase-Protein, dass hauptsächlich im „high-density“ Lipoprotein (HDL) akkumuliert und die endogen entzündungshemmende Funktion von HDL reduziert. SAA aktiviert verschiedene Rezeptorklassen in vaskulären und inflammatorischen Zellen, u.a. „toll-like“ Rezeptoren (TLR) 2 und 4.

Der erste Teil der Studie hat zum Ziel, die Signalwege von SAA in Makrophagen zu studieren, hier insbesondere für die pro-inflammatorischen Zytokine IL-1β, IL-6 und MCP-1, sowie die Nitrit- und ROS-Produktion. Die SAA-induzierte Zytokin-, Nitrit-Produktion ist in Makrophagen TLR2 und TLR4 vermittelt. Die IL-1ß Produktion ist intrazellulär über eine Aktivierung des NLRP3-Inflammasoms reguliert, wohingegen die Antagonisierung des NLRP3 Inflammasoms keinen Effekt auf die SAA-induzierte wurde in den Downstream-Pathway-Nachweis einbezogen. Laut dieser Studie IL-6, MCP-1 und Nitrit-Produktion zeigte.

Da die SAA Plasmakonzentration bei CNI-Patienten durch eine regelmäßige Dialysebehandlung nicht effizient gesenkt werden kann, sollten im zweiten Teil dieser Studie Methoden zur Entfernung von SAA aus dem Blutkreislauf untersucht werden. CytoSorb™ adsorber erwies sich als vielversprechendes Material zur Entfernung von SAA aus Plasma.

Abstract

The inflammatory environment in patients with chronic kidney disease (CKD) is a risk factor for vascular comorbidities. To date, several biomarkers have been identified in CKD patients; where one of it is serum amyloid A (SAA). SAA is an acute-phase protein that accumulates mainly in the high-density lipoprotein (HDL) and reduces the endogenous anti-inflammatory function of HDL. SAA activates various receptor classes in vascular and inflammatory cells, such as Toll-like receptors (TLRs) 2 and 4.

The first part of the study aims to investigate the signaling pathways of SAA in macrophages, in particular for the proinflammatory cytokines IL-1β, IL-6 and MCP-1, as well as nitrite and ROS production. The SAA-induced cytokines, nitrite production are mediated in macrophages via TLR2 and TLR4. IL-1β production is regulated intracellularly via activation of the NLRP3 inflammasome, whereas an antagonist of the NLRP3 inflammasome has no effect on SAA-induced IL-6, MCP-1 and nitrite production.

Because SAA plasma concentrations in CKD patients cannot be effectively reduced by regular dialysis treatment, the second part of this study explored methods for removing SAA from the bloodstream. The CytoSorb^{TM} adsorber proved to be a promising material for removing SAA from plasma.

1 Introduction

Chronic kidney disease (CKD) is one of the fastest growing causes of death worldwide in the past decade[1]. In addition, an inflammatory environment, which contributes to the increased mortality has been described for CKD patients[2,3]. Studies in recent years have shown great interest in the mechanism behind this inflammatory state. A proinflammatory protein named serum amyloid A (SAA) was found contribute to this situation. In CKD patients, SAA increases to a moderate level (10-30-fold increase). With this increase, SAA replaces of Apolipoprotein A I (apoA-I) and subsequently modifies the component, impairs the anti-inflammatory function of high-density lipoprotein (HDL)[4,5]. The HDL function impairment by SAA has been well demonstrated in a multicenter and long-term follow-up study[6]. This study recruited approximately 9,000 subjects including CKD patients. In patients with high SAA levels, the HDL level positively correlated with all- and cardiovascular-cause mortalities, while in normal-SAA-level patients, the HDL concentration negatively associated with these two mortalities. In addition to modifying the HDL component, SAA itself acts as a proinflammatory mediator and induces cytokine and chemokine expression in different cells. Given the critical role of SAA in the inflammatory response, the detailed mechanism of SAA pathogenicity needs to be explored and better understood.

1.1 SAA physiology

SAA is an acute phase reaction protein which increases over 1000-fold during acute phase responses[7]. There are four isotypes of human SAA, which are SAA1, SAA2, SAA3 and SAA4. SAA4 is considered as a constant SAA (C-SAA) due to its continuous and extensive expression[8], while human SAA3 has only been found in mammary gland epithelial cells at the transcriptional level[9]. In acute phase responses, SAA1 and SAA2 contribute to the major increase in SAA in the circulation (increases from 1-2 µg/ml to 1 mg/ml).

SAA is mainly synthesized in the liver but its expression is also found in other cells and organs, especially under inflammatory conditions[10]. The production of A-SAA is a synergistic with that of several cytokines. The A-SAA gene is required for full induction by IL-1 and IL-6[11]. IL-1 is the leading cytokine to induce SAA, followed by IL-6, TNF-α and glucocorticoids[12-14]. The negative transcriptional regulation of SAA production also has been found in mouse and human[15,16].

After its release into the circulation, SAA associates with HDL as an apolipoprotein, predominantly with HDL_3. In addition, SAA can also associate with low-density lipoprotein (LDL) and very-low-density lipoprotein (VLDL)[17]. In acute phase responses, the SAA/total HDL protein ratio can rise from 1/2 to 50[18]. With this upsurge, SAA displaces apoA-I from HDL and becomes the major apolipoprotein of HDL[19]. The binding site for SAA in HDL is still not clear. One study found that SAA binds to lipoproteins by a hydrophobic surface formed by two alpha-helical structures in the N-domain[20]. In plasma, A-SAA has a short half-life, only lasting 1-2 h and is mainly degraded by the liver and kidney[21,22]. Cells such as monocytes and mast cells can also decrease SAA levels in the circulation[23,24]. Under inflammatory conditions, SAA is degraded less efficiently[24,25]. A genetic polymorphism also contributes to the different degradation rates of SAA[26].

Figure 1 shows the physiological process of SAA introduced above. According to this diagram, SAA further induces cytokines mediating a positive feedback inflammatory reaction. The proinflammatory properties of SAA are addressed in the next section.

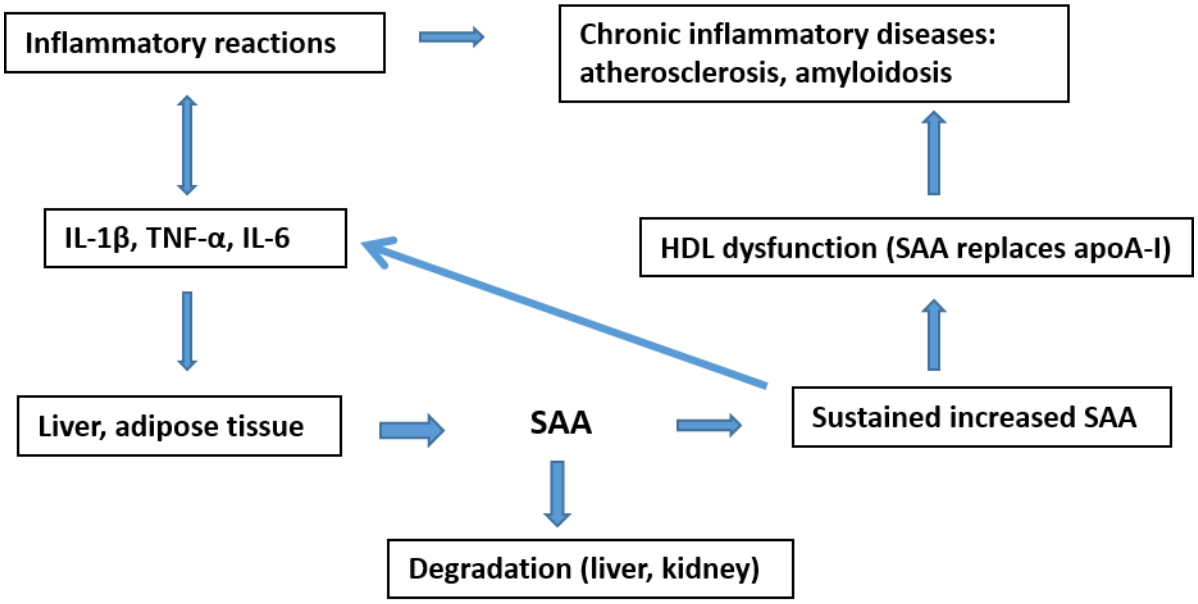

Figure 1 Physiological process of SAA
apoA-I, Apolipoprotein A I; HDL, high-density lipoprotein; IL, interleukin; SAA, serum amyloid A; TNF-α, tumor necrosis factor-α.

1.2 The biofunction of SAA

The function of C-SAA is not well known, but both pro- and anti-inflammatory properties of A-SAA have been revealed. Therefore, the following discussion regarding SAA is only about A-SAA. The anti-inflammatory function of SAA includes enhancing the opsonization of gram-negative bacteria[27,28] and neutrophil migration[29], inhibiting hepatitis C virus entry into hepatocytes[30,31], inducing retinol binding protein[32] and M2 macrophage differentiation[33], and suppressing antibody production[34]. On the other hand, SAA plays a more critical role in the immune response as an inflammatory mediator. As shown in Figure 1, SAA-induced cytokines can further promote SAA generation. This mutual induction process leads to an enhanced and sustained inflammatory reaction. In addition, SAA can also maintain this reaction by impairing the anti-inflammatory function of HDL. After enrichment with SAA, HDL loses its ability to inhibit inflammatory mediators such as MCP-1, IL-1, IL-6 and reactive oxygen species (ROS)[4,5]. Furthermore, SAA induces angiogenesis by upregulating intercellular adhesion molecule 1 (ICAM-1) and vascular cell adhesion molecule-1 (VCAM-1)[35,36], which are components of inflammation.

1.3 Receptors for SAA mediating inflammatory reaction

SAA binds to receptors from different families (Figure 2) including scavenger receptor class B type 1 (SR-BI), receptor for advanced glycation end products (RAGE), P2X purinoceptor 7 ($P2X_7$), N-formyl peptide receptor 2 (FPR2), cluster of differentiation 36 (CD36) and Toll-like-receptor 2 and 4 (TLR2/TLR4). These receptors can mediate distinct functions in cells. For instance, SR-BI is an HDL receptor that mediates cellular selective cholesterol ester uptake from HDL[37]. CD36 also belongs to the class B scavenger receptor family and can import fatty acids inside cells[38]. RAGE is a transmembrane multiligand receptor belonging to the immunoglobulin superfamily and plays a remarkable role in the pathogenesis of nephropathy[39]. FPR2 is a G protein-coupled receptor that recognizes N-formyl peptide (e.g., from bacteria) and mediates the immune response in phagocytes[40]. $P2X_7$ is an ATP-gated ion channel that allows ion transcellular movement when activated by agonists[41]. Finally, both TLR2 and TLR4 are from the TLR family and recognize molecules that are broadly shared by pathogens, which play critical roles in host immune defense. Interestingly, all these diverse receptors can act as SAA receptors and mediate cytokine production (Table 1).

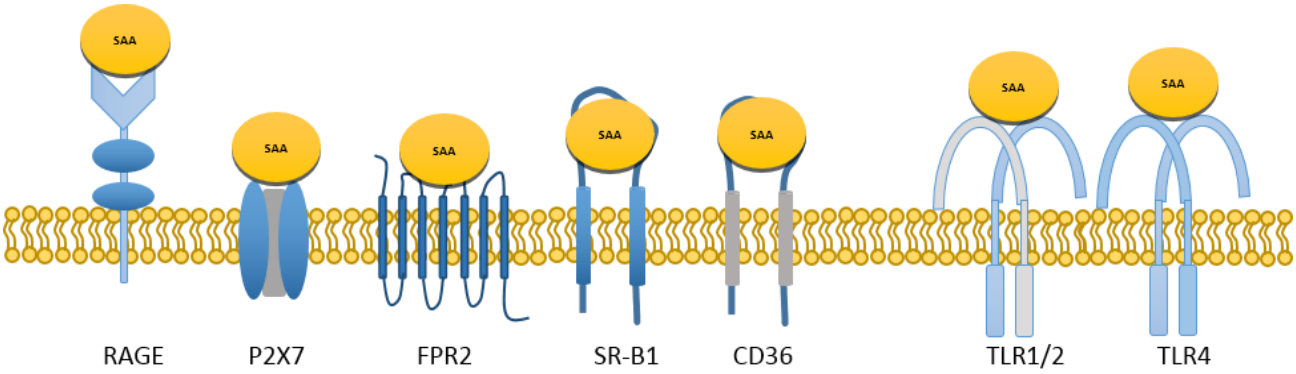

Figure 2 Receptors for SAA
SR-BI, scavenger receptor class B type 1; RAGE, receptor for advanced glycation end products, $P2X_7$, P2X purinoceptor 7; FPR2, N-formyl peptide receptor 2; CD36, cluster differentiation 36; TLR2/TLR4, Toll-like-receptor 2 and 4.

Table 1 Receptors and pathways for SAA-mediated inflammatory reactions

Receptors	Target cells	Activated pathway	Induced cytokines and other proteins	References
TLR2	Human monocytes	CK-1, NF-κB	G-CSF	[42]
	Mouse macrophages THP-1 monocytes and PBMCs	IRF-7, TRAF6	IL-33	[43]
	Coronary artery endothelial cells	JNK, ERK, NF-κB (p65, p105)	IL-6, IL-8, G-CSF, GM-CSF, ICAM-1 and VCAM-1	[36]
	Skeletal muscle cells	NA	TNF-α, IL-6	[44]
	Microvascular endothelial cells	NF-κB	ICAM-1, IL-8, MCP-1, RANTES and CXCL1	[35]
	Dermal fibroblasts	IRAK4, NF-κB	IL-6	[45]
	HeLa cells	ERK, p38 MAPK, and JNK	IL-10	[46]
	γδ T cells	NA	IL-17	[47]
TLR2/TLR4	Keratinocytes	NLRP3, caspase-1, NF-κB	IL-1β	[48]
	Mouse macrophages THP-1 macrophages	NLRP3	IL-1β	[49]

Table 1 (continued)

TLR4	Mouse macrophages	NA	HMGB1	[50]
	Fibroblast-like synoviocytes and chondrocytes	NA	IL-6, IL-8, CXCL1 and MCP-1	[51]
	Mouse macrophages	MD-2, MyD88, p38 MAPK, JNK, Akt	IL-6	[52]
FPR2	Human neutrophils	ERK1/2, p38 MAPK, NF-κB	IL-8	[53]
		NA	IL-6	[54]
	Mouse airway epithelial cells	NA	IL-8	[55]
	Vascular smooth muscle cells	NA	MCP-1	[4]
SR-BI	Rheumatoid arthritis synovial membrane	NA	IL-6, IL-8	[56]
	Synovial explant cultures	NA	MMP-2, and MMP-9 TNF-α	[57]
RAGE	Fibroblast-like synovial cells	NF-κB	IL-6 and IL-8	[58]
$P2X_7$	Mouse macrophages, THP-1 macrophages	NLRP3	IL-1β	[49]
CD36	Rat macrophages	JNK and ERK1/2	IL-8	[59]

NA, data not available; CD36, cluster of differentiation 36; CK-1, casein kinase 1; CXCL 1, chemokine ligand 1; ERK, extracellular signal–regulated kinases; FPR2, formyl peptide receptor 2; G-CSF, granulocyte colony-stimulating factor; GM-CSF, granulocyte-macrophage colony-stimulating factor; HMGB1, high mobility group box 1; ICAM-1, intercellular adhesion molecule 1; IL, interleukin; IRF-7, interferon regulatory factor 7; JNK, c-Jun N-terminal kinases; MAPK, Mitogen-activated protein kinase; MCP-1, monocyte chemoattractant protein 1; MMP, matrix metalloproteinase; MyD88, Myeloid differentiation primary response 88; NF-κB, nuclear factor kappa-light-chain-enhancer of activated B cells; PBMCs, peripheral blood mononuclear cells; $P2X_7$, P2X purinoceptor 7; RAGE, receptor for advanced glycation end products; SR-BI, scavenger receptor B1; TLR, Toll like receptor; TNF-α, tumor necrosis factor alpha; TRAF6, TNF receptor associated factor 6; VCAM-1, vascular cell adhesion molecule-1.

1.4 Proinflammatory cytokines induced by SAA and the signaling pathways involved

SAA (Table 1) can induce different cytokines through distinct receptors in diverse cell types. Among those cytokines, IL-1β can be upregulated very quickly, e.g., lipopolysaccharide (LPS) can increase IL-1β mRNA within 15 min and peak at 4 h[60]. After release from the cells, IL-1β binds to the IL-1β receptor and promotes the secretion of other cytokines such as TNF-α and IL-6[61], and self-induced IL-1β secretion as well[62]. IL-1β is mainly released from

monocytes and macrophages, in which its synthesis is stimulated upon the recognition by pattern recognition receptors (PRRs) of pathogen-associated molecular patterns (PAMPs) or damage-associated molecular patterns (DAMPs)[63]. IL-1β secretion is a two-step process that includes priming and activation. For instance, LPS can only prime cells and induce pro-IL-1β rather than mature IL-1β[64]. The pro-IL-1β must to be further cleaved by caspase-1, which is activated by the NOD-like receptor, pyrin domain containing 3 (NLRP3) inflammasome, to finally be released as mature IL-1β[65]. During this unique and complicated process, in addition to the stimulation of PRRs, other activators might be indispensable for the production of mature IL-1β, e.g., extracellular adenosine triphosphate (ATP) is a NLRP3 inflammasome activator required for the LPS-stimulated IL-1β secretion[66]. The NLRP3 inflammasome can also be activated by potassium (K^+) efflux, calcium (Ca^{2+}) influx, ROS and mitochondrial dysfunction[65]. On the other hand, NLRP3 inflammasome- or Caspase-1-independent IL-1β release has also been demonstrated in knockout mice[67]. Several studies have investigated the pathway for SAA-induced IL-1β. According to those research studies, SAA-induced IL-1β is NLRP3 inflammasome-caspase-1-dependent[49,68]. Furthermore, unlike LPS, no extra activator is required for SAA processing of IL-1β maturation[69], possibly owing to the multireceptor activation by SAA. TLR2 and TLR4 are the two SAA receptors that promote IL-1β secretion[48]. However, these two receptors are involved in the priming step, which upregulates pro-IL-1β and NLRP3[48]. The mechanism by which SAA activates the NLRP3 inflammasome and releases IL-1β is still unclear. $P2X_7$ is an ATP-gated ion channel, that can release mature IL-1β via K^+ efflux[66]. Thus, the role of this receptor in SAA-induced IL-1β has been investigated. However, two studies reached contradictory conclusions[65,68]. Another possible activator for SAA-mediated IL-1β maturation are ROS. The inhibition of ROS blocked IL-1β secretion in SAA-stimulated macrophages[68], whereas another study indicated an increase in SAA-induced IL-1β production by mitochondrial-targeted drugs regardless of the ROS level[69]. Considering the inconsistent results, more investigations are needed to clarify these questions.

In addition, IL-6, one of the major inducers of hepatic acute phase protein, is a cytokine that can be induced by SAA in diverse cells. IL-6 was initially found in monocytes and macrophages after LPS stimualtion[70]. The IL-6 biofunctions include facilitating the differentiation of $CD8^+$ T cells to cytotoxic T cells and B cell antibody secretion, and promoting

vascular permeability and angiogenesis[71]. Different receptors are involved in SAA-induced IL-6 secretion in different cell types. For example, SAA upregulates IL-6 in coronary artery endothelial cells and skeletal muscle cells via TLR2[36,44], while in fibroblast synovial cells and mouse macrophages, SAA promotes IL-6 secretion through TLR4[51,52]. SR-BI and RAGE also act as the SAA receptors to induce IL-6 in rheumatoid arthritis synovial membranes and fibroblast-like synovial cells[56,58].

Moreover, MCP-1 is one of the most important SAA-induced chemokines, and plays a pivotal role in monocyte recruitment during inflammatory reactions. Due to this feature, MCP-1 participates in bone remodeling, central nervous system (CNS) inflammation development and atherosclerotic lesion formation[72]. In atherosclerosis, the accumulated SAA can induce local inflammation by upregulating MCP-1 in monocytes and macrophages[73]. TLR2, TLR4 and FPR2 have been demonstrated as receptors for SAA that mediate MCP-1 secretion[4,35,51].

As discussed before, IL-1β is an early response cytokine, that subsequently induces the generation of IL-6 and the other cytokines. The significantly reduced IL-6 found in IL-1β-deficient mice is indicative of the IL-1β-dependent IL-6 synthesis[61]. While a recent study demonstrated different regulations of IL-1β and IL-6 in murine macrophages, showing that in J774.1 and RAW 264.7 cells, LPS and ATP failed to process pro-caspase-1 and pro-IL-1β to their mature forms, the release of IL-6 was not affected[74]. Similarly, a NF-κB-binding site in the MCP-1 gene was found to be a critical element in MCP-1 induction in response to IL-1β[72]. Accordingly, these SAA-induced cytokines might interact with each other to maintain the immune response.

In summary, TLR2 and TLR4 serve as the most significant receptors for SAA to induce the production of proinflammatory mediators. IL-6, IL-1β and MCP-1 are the major SAA-stimulated cytokines. The intracellular signaling pathway after TLR2/TLR4 activation includes the receptor adaptor MyD88, protein kinase MAPK and transcription factor NF-κB (Table 1). NLRP3-caspase-1 can also be activated by SAA and mediates IL-1β release[48]. The interconnections between these signaling pathways and SAA-induced cytokines have not been well studied and need to be investigated in the future.

1.5 ROS and NO induced by SAA

ROS are a group of reactive chemical species containing oxygen that are generated through NADPH oxidase 2 (NOX2)-dependent and independent pathways. Depending on the source, ROS can be classified as mitochondrial-derived ROS and intracellular-generated ROS. Among all the ROS forms (including hydrogen peroxide, hydroxyl radicals, hypochlorous acid, anion hypochlorite, and superoxide anion radical), superoxide anion radical is a short-lived but key precursor of other ROS forms in cells[75]. Classically, ROS are considered host defense molecules released by neutrophils to kill pathogens such as bacteria. In addition, ROS can toxic to the cell. For instance, hydroxyl radicals remove hydrogen atoms from lipids, nucleic acids, and proteins, which yields the formation of reactive radicals and finally results in cell death. This cytotoxicity contributes to the pathological processes of atherosclerosis, diabetes and inflammation[76,77]. In recent years, numerous studies have demonstrated that ROS are not only the products of cellular reactions but are also mediators for multiple cell signal transductions[78], such as the activation of NLRP3 inflammasomes[79].

SAA can induce both intracellular ROS and mitochondrial ROS[69,80]. However, the sources of these ROS were shown to be controversial in two studies. In fibroblasts, the SAA-induced ROS was NADPH dependent[80], whereas in another study in macrophages, diphenyliodonium (DPI) (NADPH inhibitor) promoted more ROS than inhibited ROS production[69]. The SAA-induced ROS were found to participate in NLRP3 activation[68,69]. Other biofunctions of SAA-induced ROS need to be explored.

Nitric oxide (NO) also belongs to free radicals and is a critical cell signaling molecule. The three NO synthase (NOS) systems, according to the original tissues in which they were first described, are named endothelial NOS (eNOS), neuronal NOS (nNOS) and inducible NOS (iNOS). NO generated from different NO synthases can have distinct effects. For example, eNOS-generated NO plays a protective role in the cardiovascular system by inhibiting smooth muscle cell proliferation, endothelial apoptosis and cell adhesion, and suppressing platelet aggregation[81]. As its name suggests, iNOS is inducible and can regulate the immune response[82]. The upregulation of iNOS in macrophages contributes to acute lung injury, insulin resistance, intestinal neuron damage, and tumor cell survival[83-86]. iNOS also plays a role in the progress of atherosclerosis by inhibiting macrophage-derived foam cell migration[87]

and promoting carotid plaque vulnerability via NF-κB activating[88]. Interestingly, SAA decreases eNOS in human aortic endothelial cells[89] but upregulates iNOS in murine macrophages[90]. The reduced eNOS and increased iNOS can both lead to adverse outcomes of the cardiovascular system. Thus, there is an outstanding necessity to investigate mechanisms for SAA-induced NO production.

1.6 Blood purification methods and their ability to remove solutes

Considering the proinflammatory property of SAA and the association found between this protein and CKD[2,91], remove SAA from bloodstream might be a promising therapy option for CKD patients.

Different blood purification methods designed to remove certain substances from the blood are available in the clinic. Hemodialysis (HD) and hemofiltration (HF) are the two major renal replacement therapies. HD is a diffusion method, in which the molecular movement of solutes is achieved by a concentration difference. The first generation of HD units had a good ability to remove low-molecular-weight uremic toxins such as urea and creatinine. After more medium- to high-molecular-weight uremic solutes were identified in CKD[92], second generation materials such as high-flux membranes with increased permeability were developed. The high-flux membrane has a better dialysis adequacy which can remove substance with molecular mass in the range of 2-50 kD (compared to 2-15 kD for low-flux or general membranes)[93]. However, no consistent conclusion has been reached regarding the benefit of this new material in different clinical settings. During HF treatment, medium-molecular weight solutes are removed by the movement of fluid in response to an osmotic force. This therapy is more frequently applied in acute kidney failure patients and is usually combined with HD, which is referred to as hemodiafiltration (HDF). Standard HF has limitations in the removal of inflammatory toxins[94]. By increasing plasma-water exchanges, high-volume HF (HVHF) can remove inflammatory mediators from plasma. However, no improvement in survival was found in sepsis patients receiving HVHF treatment when compared to those receiving standard dialysis[95]. Based on the ability of HF to remove middle-molecular-weight solutes, a high cut-off (HCO) membrane has been developed to eliminate inflammatory mediators. The HCO membrane shows the potential to remove cytokines (which have a molecular mass of up to 60 kDa), although, questions regarding timing,

duration, and molecular weight cut-off need to be further addressed[96]. Unlike the membrane-based technology applied in HD and HF, hemoadsorption places sorbents in direct contact with blood and has the ability to adsorb high-molecular-weight substances. CytoSorb™ adsorber is a kind of biocompatible bead designed to remove pro- and anti-inflammatory mediators with molecular weight of 5-60 kDa. Studies have shown a notable reduction of in cytokines such as IL-6, IL-8, TNF-α, and CCL2 and pathogen-associated molecular patterns within several hours of CytoSorb™ adsorber treatment[97,98]. However, none of the above studies have reported the effect on SAA level during treatment.

1.7 Aim of the study

Given the critical role of SAA in the sustained inflammatory reaction that contributes to the mortality and cardiovascular complications of CKD patients, it is necessary to explore the detailed mechanisms behind this. In atherosclerosis, macrophages are activated by danger ligands such as oxidized LDL (oxLDL), which consequently leads to the production of proinflammatory cytokines that results in disease progression[99]. Elevated SAA can also be a danger ligand for macrophages, but the subsequent reactions are still not clear. Therefore, there are two aims in the first part of this study. One is to confirm the ability of SAA to induce proinflammatory mediators including IL-1β, IL-6, MCP-1, nitrite production and ROS in macrophages. Another is to investigate signaling pathways for these SAA-induced reactions. Since TLR2 and TLR4 serve as the best receptors for SAA, these two receptors were included in this study. The NLRP3 inflammasome has been found to participate in SAA-induced IL-1β release, but no information is available regarding the role of the NLRP3 inflammasome in the generation of other cytokines. Therefore, the NLRP3 inflammasome was investigated as the intracellular signaling pathway for SAA-mediated cytokine production.

Our previous research has demonstrated that the SAA concentration can reach 300 μg/ml in dialysis patients. How to remove SAA from the blood is a completely unknown question. The molecular weight of SAA is 11.4-12.5 kDa, which means that HDL-free SAA can be eliminated by HD and HF. After the association of SAA with HDL in the circulation, the molecular weight of SAA-HDL is more than 300 kDa. This explains the low clearance rate of

SAA in regular dialysis. The purpose of the second part of this study is to explore methods for removing SAA from the bloodstream.

2 Materials and methods

2.1 Manufacturer information on regents, devices and software

Table 2 Materials for cell culture

Medium and materials for cell culture	Manufacturer
Dulbecco's modified Eagle's medium (DMEM)	Biochrom AG, Berlin, Germany
Fetal bovine serum (FBS)	Biochrom AG, Berlin, Germany
L-glutamine	Biochrom AG, Berlin, Germany
Penicillin/streptomycin	Biochrom AG, Berlin, Germany
Phorbol 12-myristate 13-acetate (PMA)	Sigma, MO, USA
Roswell Park Memorial Institute (RPMI) 1640	Biochrom AG, Berlin, Germany

Table 3 Agonists and antagonists

Receptors	Agonists	Manufacturer	Antagonists	Manufacturer
Toll-like receptor 4 (TLR4)	Lipopolysaccharides (LPS)	InvivoGen, San Diego, USA	TAK-242	InvivoGen, San Diego, USA
Toll-like receptor 2 (TLR2)	-	-	CU CPT22	Tocris, MO, USA
NLRP3 inflammasome	-	-	MCC950	InvivoGen, San Diego, USA
TLR2/TLR4	SAA	PeproTech, Hamburg, Germany	-	-

Chemical formulas: TAK-242, $C_{15}H_{17}ClFNO_4S$; CU CPT22, $C_{19}H_{22}O_7.H_2O$; MCC950, $C_{20}H_{24}N_2O_5S$

Table 4 Regents for qRT-PCR

	Regents	Manufacturer
mRNA isolation	RLT Buffer	QIAGEN, Venlo, Netherlands
	ß-mercaptoethanol	
	RNeasy Kit	
cDNA synthesis	RT-Buffer	ThermoFisher Scientific, USA
	dNTP's	ThermoFisher Scientific, USA
	Random Primer	ThermoFisher Scientific, USA
	MultiScribe RT	Bio-Rad, CA, USA
PCR	iQ SYBR Green Supermix	Bio-Rad, CA, USA
	Primers	TIB Molbiol, Berlin, Germany

Table 5 Other regents

Regents	Manufacturer
CellTiter 96® Aqueous One Solution Cell Proliferation Assay	Promega, Madison, USA
CytoTox-Glo™ Cytotoxicity assay	Promega, Madison, USA
Diagnostic reagent for lipids and lipoproteins	DiaSys, Diagnostic Systems GmbH, Germany
DiaSys Diagnostic Systems	GmbH, Holzheim, Germany
Griess Reagent System	Promega, Madison, USA
Human serum amyloid A (Hu SAA) ELISA Kit	ThermoFisher Scientific, USA
MILLIPLEX® MAP Human Cytokine/Chemokine Magnetic Bead Panel	Merck KGaA, Darmstadt, Germany
NP40 cell lysis buffer	Invitrogen, CA, USA
Pierce™ BCA Protein Assay	ThermoFisher Scientific, USA

Table 6 Materials used in CytoSorb™ experiment

Materials	Manufacturer
CytoSorb™ adsorber	CytoSorbents Europe GmbH, Berlin, Germany
Heidelberger Extension	Fresenius Kabi AG, Germany
Pump tube	IDEX Health & Science, Germany
Pump	ISMATEC, Germany
1 ml Column	SUPELCO, Germany
595 Filter paper	GE Healthcare Life Science, Germany

Table 7 Devices and software

Devices	Manufacturer	Software	Manufacturer
Plate reader	Multiskan Spectrum, ThermoFisher Scientific, USA	Bio-Plex Manager software 4.1	Bio-Rad, CA, USA
Mithras plate reader	Berthold Technologies, Germany	GraphPad Prism statistical software v6.0	GraphPad, CA, USA
Bio-Plex 100	Bio-Rad, CA, USA	BioRad CFX Manager Software 3.1	Bio-Rad, CA, USA
Bio-Rad T100 and C1000 Thermal Cycler	Bio-Rad, CA, USA	-	-
QiaCube	QIAGEN, Venlo, Netherlands	-	-

2.2 Cell culture

2.2.1 THP-1 cell culture and differentiation

THP-1 cells were purchased from American Type Culture Collection (Manassas, VA, USA) and were stored in cryovials in liquid nitrogen in 90% FBS and 10% dimethyl sulfoxide (DMSO). Cells were defrosted with a fast warm up in a 37°C water bath until just defrosted. Then, the cells were quickly transferred into prewarmed media and centrifuged at 2,000 rpm for 5 min. Cells were cultured in RPMI-1640 (2 mM L-glucose) medium supplemented with 10% FBS and 1% antibiotic (penicillin/streptomycin) in 75 cm^2 culture flasks at 37°C with 5% CO_2. Cell density was maintained at approximately 1×10^6 cells/ml during culture. THP-

1 monocytes were differentiated into macrophage-like cells by treatment with 200 µg/ml PMA for 24 h.

2.2.2 RAW 264.7 cell culture

The company source, the storage conditions, and the cell defrosting procedure are all the same as for THP-1 cells. DMEM medium (4.5 g/L D-glucose) supplemented with 10% FBS and 1% antibiotic (penicillin/streptomycin) was used for RAW 264.7 cell culture. The incubator conditions were also set as 37°C with 5% CO_2. Cells were split when they reached approximately 80% confluency. Cells were dislodged from the flasks by using a cell scraper.

2.3 Quantitative RT-PCR

qRT-PCR was performed to quantify TLR2 and TLR4 mRNA levels. THP-1 monocytes and macrophages were serum starved in flasks for 24 h, and the total mRNA was extracted from the cells using the RNeasy Kit from Qiagen according to the manufacturer's protocol. The procedure was run by QiaCube or by hand. Briefly, cells were washed by twice ice-cold PBS, and then groups of 1×10^6 cells were lysed in 350 µl RLT Buffer with 1% β-mercaptoethanol. After cryopreservation at -80°C for 2 h, the mRNA was extracted by several short centrifugations after each kit was added to the RNeasy spin column, and then the mRNA was washed down from spin columns with 50 µl RNase-free water into collection tubes. Afterward, cDNA was synthesized from mRNA using random primers. The reaction conditions were 10 min at 25°C, and 2 h at 37°C. Finally, each target and housekeeper gene was quantified by PCR using designed primers (Table 8). The reaction volume in each well (384 well-plate) was 10 µl, with 3 µl (4.5 µg) cDNA, 0.8 µl of primers (0.4 µl forward and 0.4 µl reverse 10 µM primers), and 6.2 µl iQ SYBR Green Supermix (5 µl Supermix and 1.2 µl water). The PCR conditions were as follows: initial denaturation for 3 min at 95°C, denaturation for 15 sec at 95°C for 39 cycles, primer annealing for 15 sec at 60°C, and DNA extension for 1 min at 72°C. Data were analyzed by Bio-Rad CFX Manager Software 3.1. The results were verified by running amplified cDNA on a 2% agarose gel.

Table 8 Primers for PCR

Species	Gene	Sequence	Amplicon [bp]
Human	ß-Actin	fwd: 5´- AAC CCC AAG GCC AAC CGC GAG AAG ATG ACC - 3´	415
		rev: 5´- GGT GAT GAC CTG GCC GTC AGG CAG CTC GTA - 3´	
Human	GAPDH	fwd: 5´- CATGGGTGTGAACCATGAGAA - 3´	132
		rev: 5´- GGTCATGAGTCCTTCCACGAT - 3´	
Human	TLR2	fwd: 5' - GGC CAG CAA ATT ACC TGT GT - 3'	320
		rev: 5' - CTC CAG CTC CTG GAC CAT AA - 3'	
Human	TLR4	fwd: 5' - GGT GGG AAT GCT TTT TCA GA - 3'	358
		rev: 5' - AAT TGC CAG CCA TTT TCA AG - 3'	

Fwd, forward primer; rev, reverse primer; GAPDH, glyceraldehyde-3-phosphate dehydrogenase; TLR, Toll-like receptor.

2.4 Assays

2.4.1 BCA assay

BCA Protein Assay is a method that combines the reduction of $Cu2^{+}$ to Cu^{1+} by protein with the colorimetric detection using a reagent containing bicinchoninic acid. The reaction is shown in Figure 3. The working range for the standard protocol is 20-2000 µg/ml protein. Samples with an estimated concentration higher than 1500 µg/ml were prediluted with PBS. The test was run according to the protocol. Summarized as working reagent preparation (50 parts of BCA Reagent A with 1 part of BCA Reagent B), samples and working reagent mixing, and a 30 min at 37°C incubation. Finally, read plates at 560 nm. The results were calculated by adjusting to the standard curve.

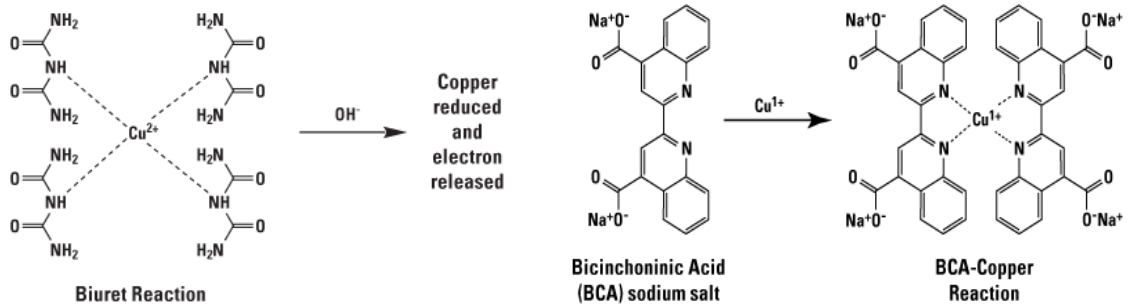

Figure 3 Bicinchoninic acid assay reaction
(https://www.thermofisher.com/de/de/home/life-science/protein-biology/protein-biology-learning-center/protein-biology-resource-library/pierce-protein-methods/chemistry-protein-assays.html)

2.4.2 Proliferation assay

Cell proliferation was determined by CellTiter 96® Aqueous One Solution Cell Proliferation Assay (MTS), which is a colorimetric method for determining the number of viable cells. First, 0.5 × 10^5 cells/well of THP-1 macrophages were seeded in 96-well plates for 24 h with serum starvation first. Then, the cells were stimulated cells for 24 h with different concentrations of drugs. To summarize, next 20 µl CellTiter One Solution Reagent was added into each well, the cells were incubated at 37°C and 5% CO_2 for 30-60 min until the medium color turned between yellow and dark brown, and finally the absorbance at 490 nm was determined. The results were analyzed by normalizing absorbance to the control group and calculating the percentage of viable cells in stimulated groups.

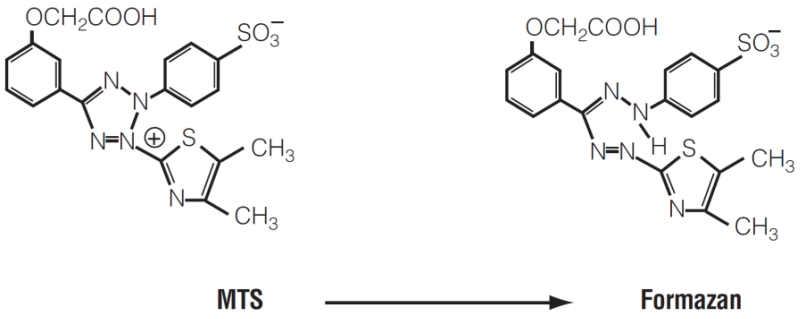

Figure 4 Structures of MTS tetrazolium and its formazan product
(https://www.promega.com/-/media/files/resources/protocols/technical-bulletins/0/celltiter-96-aqueous-one-solution-cell-proliferation-assay-system-protocol.pdf)

2.4.3 Cytotoxicity assay

Cytotoxicity was detected by CytoTox-Glo™ Cytotoxicity assay. This assay uses luminescence to determine the number of dead cells in the cell population (Figure 5). To optimize the results, assay sensitivity was determined beforehand using different densities of THP-1 macrophages. According to the sensitivity assay results, 5,000 cells/well of THP-1 macrophages in 96-well white-wall-clear-bottom plates were employed in this assay. The stimulation was the same as in the proliferation assay. Briefly, after adding 50 µl of Cytotoxicity assay reagent to each well and incubating the cells for 15 min at room temperature, the luminescence values were determined by a Mithras plate reader. Luminescence values obtained

at this step represented the number of dead cells. Afterward, 50 µl cell lysis reagent (33 µg digitonin in 5 ml assay buffer) was added to each well, and the plate was shaken at 600 rpm for 15 min. The plate was then read for the second time. Luminescence values acquired from this step indicated the total cell number. The number of viable cells was calculated by the absorbance difference between the total cell and the dead cell measurements. The results were normalized to the control group to obtain the percentage of viable cells.

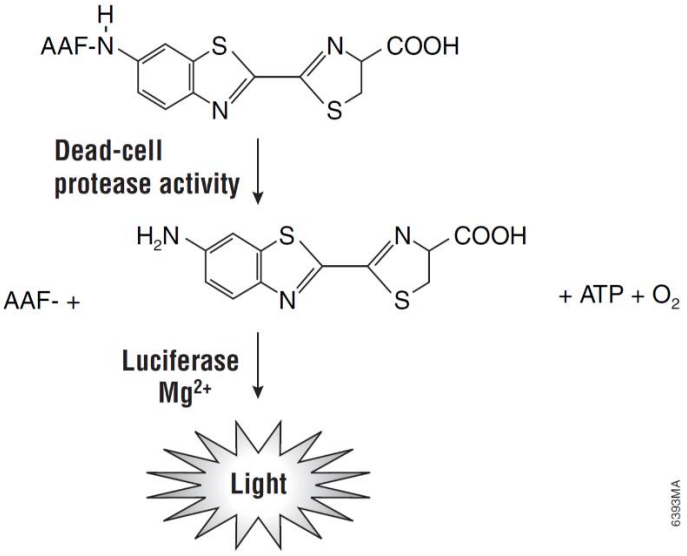

Figure 5 Cleavage of the luminogenic AAF-Glo™ Substrate by dead-cell protease activity (https://www.promega.com/-/media/files/resources/protocols/technical-bulletins/101/cytotox-glo-cytotoxicity-assay-protocol.pdf?la=en)

2.4.4 Nitrite production detection

Nitrite production was determined by Griess Reagent System, which is based on chemical reactions between NO_2^-, sulfanilamide, and *N*-1-naphthylethylenediamine dihydrochloride (NED) under acidic conditions (Figure 6). The final chemical product has an azo-compound that can be detected by a 520-550 nm filter. After 24 h of stimulation, 50 µl of supernatant from each well was collected after 10 min of centrifuge at 1,200 rpm at 4°C. The nitrite solution standard (100 µM) was set up at 6 serial 2-fold dilutions (50 µl/well) to generate a standard reference curve. Afterward, 50 µl of sulfanilamide solution was added to all experimental samples and standards. After incubating for 5-10 min at room

temperature protected from light, 50 µl NED Solution was added to each well. Then, incubation for another 5-10 min was carried out at room temperature in the dark. Finally, absorbance values were obtained within 30 min at 540 nm. Nitrite production was calculated by adjusting to the standard curve.

RAW 264.7 cells were seeded in 96-well plates and serum starved (DMEM without serum and phenol red, plus 1% glutamine and antibiotics) for 24 h before stimulation. The cell density for this experiment was 50,000 cells/well.

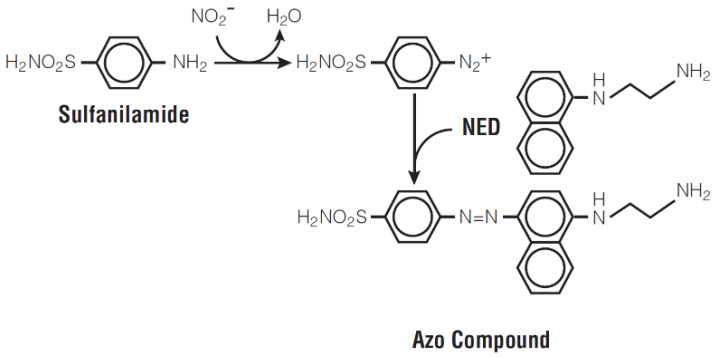

Figure 6 Chemical reactions involved in the measurement of NO_2- using the Griess Reagent System (https://www.promega.com/-/media/files/resources/protocols/technical-bulletins/0/griess-reagent-system-protocol.pdf?la=en)

2.4.5 ROS detection

Intracellular oxidants were detected by dihydroethidium (DHE). DHE can form a red fluorescent product after reacting with the superoxide anion, with maximum excitation and emission peaks at 480-520 and 570-600 nm, respectively. After stimulation, the cells were washed with warm PBS once. Then, the plate was centrifuged for 5 min at 500 × g, PBS was aspirated and 100 µl DHE working solution (5 µM) was added to each well. After 90 min incubation at 37°C (protected from light), the plate was measured by a fluorescent plate reader using an excitation wavelength of 485-530 nm and an emission wavelength of 590-620 nm.

Mitochondrial-derived ROS were measured using the MitoSOX Red fluorescent probe. This probe is similar to DHE in that it also reacts with superoxide anions but is specific for ROS production in the mitochondrial matrix. Cells were washed with

warm PBS once after stimulation. Then the plate was centrifuged for 5 min at 500 × g, PBS was aspirated and 100 µl MitoSOX Red working solution (5 µM) was added to each well. According to the manufacturer's protocol, cells were incubated for 10 min at 37°C (protected from light). Finally, the plate was measured by a fluorescent plate reader at excitation/emission wavelengths of 485-530/590-620 nm, respectively.

2.4.6 Luminex™ assay

MCP-1, IL-1β and IL-6 were detected by MILLIPLEX® MAP Human Cytokine/Chemokine Magnetic Bead Panel in a Bio-Plex 100 device, based on the Luminex™ xMAP® technology (Figure 7). THP-1 macrophages were seeded in 96-well plates and serum starved for 24 h before treatment, and 10,000 cells/well were used in this experiment. After 24 h and 48 h of stimulation, the plates were briefly centrifuged, and the supernatants were collected in 1.5 ml tubes. The Luminex™ procedures were performed strictly according to the manufacturer's instructions. Working standards were prepared for calculating cytokines concentrations, which were normalized to protein content. The protein content was determined from cell lysates. Briefly, cells were washed twice with PBS in the plate, lysed in 40 µl NP40 cell lysis buffer per well for 10 min and transferred to tubes after resuspending at least 5 times. Protein concentration was determined by BCA assay after centrifugation of the cell lysates at 10,000 rpm for 10 min. Supernatant and cell lysates were harvested on the ice. The results were analyzed by Bio-Plex Manager software 4.1.

The Luminex™ assay was also applied in SAA and C-reactive protein (CRP) measurements in the "Adsorption methods to remove SAA from plasma" experiment. Plasma samples were pre-diluted at 1:1000 and 1:500.

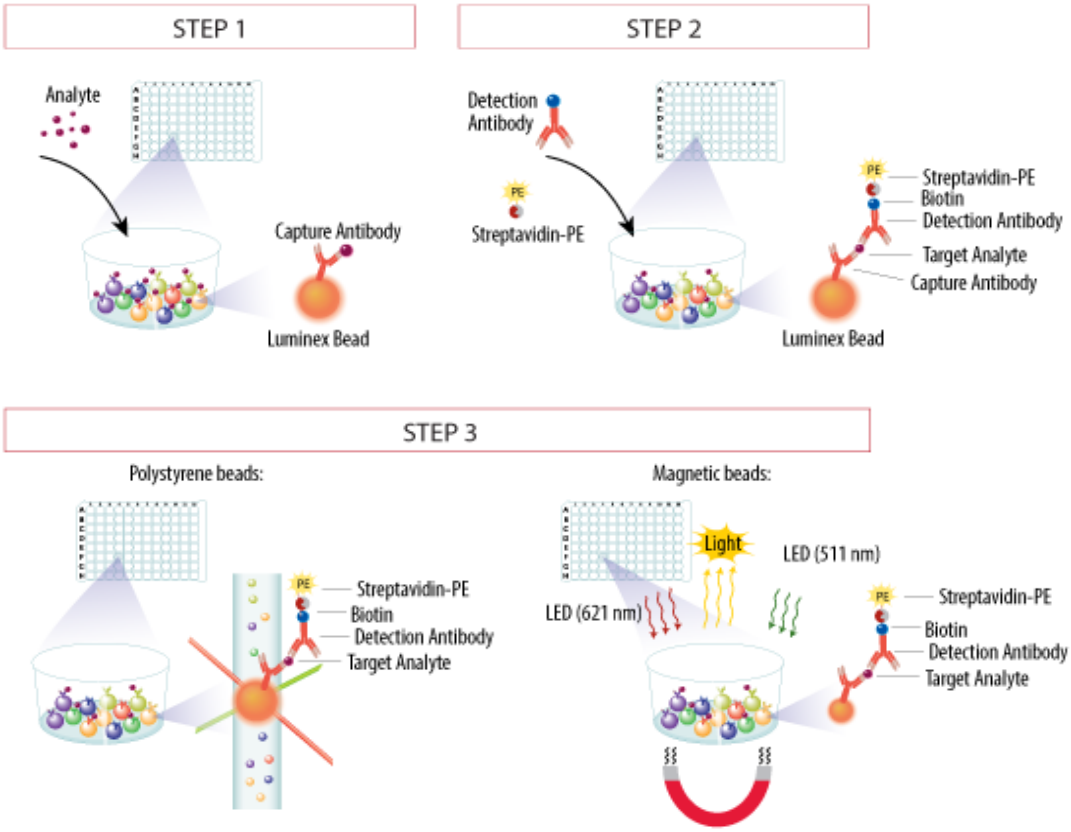

Figure 7 Luminex™ assay principle
(https://www.rndsystems.com/resources/technical/luminex-assay-principle)

Step 1: Color-coated polystyrene beads are mixed with the antibodies pre-coated by analyte-specific capture. The sample is added to this mixture. The antibodies bind to the corresponding analyte. Step 2: Detection antibodies specific to the analytes are added to form an antibody-antigen sandwich. Then phycoerythrin (PE)-conjugated streptavidin is added. Streptavidin binds to biotinylated detection antibodies. Step 3: Beads are read on a dual-laser flow-based detection instrument. One laser classifies the bead and determines the analyte. Another laser quantifies the analyte by determining the magnitude of the PE-derived signal.

2.4.7 Human serum amyloid A ELISA assay

Serum amyloid A was assessed by human serum amyloid A (Hu SAA) enzyme-linked immunosorbent assay (ELISA) kit which is a solid-phase sandwich enzyme-linked immunosorbent assay. The test range was 0-600 ng/ml. Samples were diluted by a factor from 10~10000 before measurements. The ELISA assay was run according to the manufacturer's instructions. Eight concentrations of standard from 0 to 600 ng/ml were prepared for calculating the reference standard curve. Since the standard supplied by the manufacturer was human native SAA, but the

SAA used in our research was a recombinant one, the results were adjusted to the 0 h SAA concentration.

2.4.8 Lipids and lipoprotein determination

Triglycerides, cholesterol, phospholipids, HDL-C and LDL-C were all determined by methods based on an enzymatic photometric assay. Principles for those assays are shown in Table 9.

2.5 Adsorption methods to remove SAA from plasma

To explore methods to remove SAA from the blood, a mini plasma adsorption system was established by our group. CytoSorb^{TM} adsorber and another adsorbent beads made by novel material were used in this experiment.

2.5.1 Principle and design of the experiment

Human plasma was isolated from whole blood collected in EDTA-treated tubes from healthy volunteers by centrifugation for 15 min at 2,000 × g. The main purpose of this experiment was to determine the ability of the materials to remove SAA from plasma. Thus, 31.25 μg/ml recombinant SAA was added into 10 ml serum. The control sample was serum from the same subject but without the addition of SAA. Detailed experimental settings are included in the next section. The pump running speed was set as 9. Samples from 0 h, 4 h, 24 h, 48 h and 72 h treatment points were collected for further measurements. Bead columns were replaced by new columns at 24 h intervals. SAA, lipids, lipoproteins, CRP, and total protein were all measured. The system without adsorbent beads was first tested to exclude the non-specific binding of the system, by running samples in the system without beads for 72 h.

2.5.2 Experimental settings

To construct the mini plasma adsorption system (Figure 8 A) included the following steps. During system construction, the fluid outlet tubing was ensured to be sufficiently long to reach the bottom of the tube. Materials and devices are shown in Figure 8 B.

- Prepare beads solution with PBS and adsorbent beads.

- Cut filter paper size to fit in the bead column.
- Put the filter paper into one end of the reaction vessel.
- Fill the reaction vessel with beads solution, which is the adsorbent bead column in the system. Remove all the PBS in the column by a syringe, to avoid sample dilution during treatment.
- Connect the system with infusion extension tube.
- Run the system as in Figure 8 A without a bead column to fill the system with fluid and ensure a good connection in the whole system.
- Run the system with bead column.
- The sample is running in the direction as shown in Figure 8 A, and the column is kept vertical during treatment. The filter paper side is the outlet end of the column is always at the bottom to ensure that adsorbent beads will not spill over from the column.

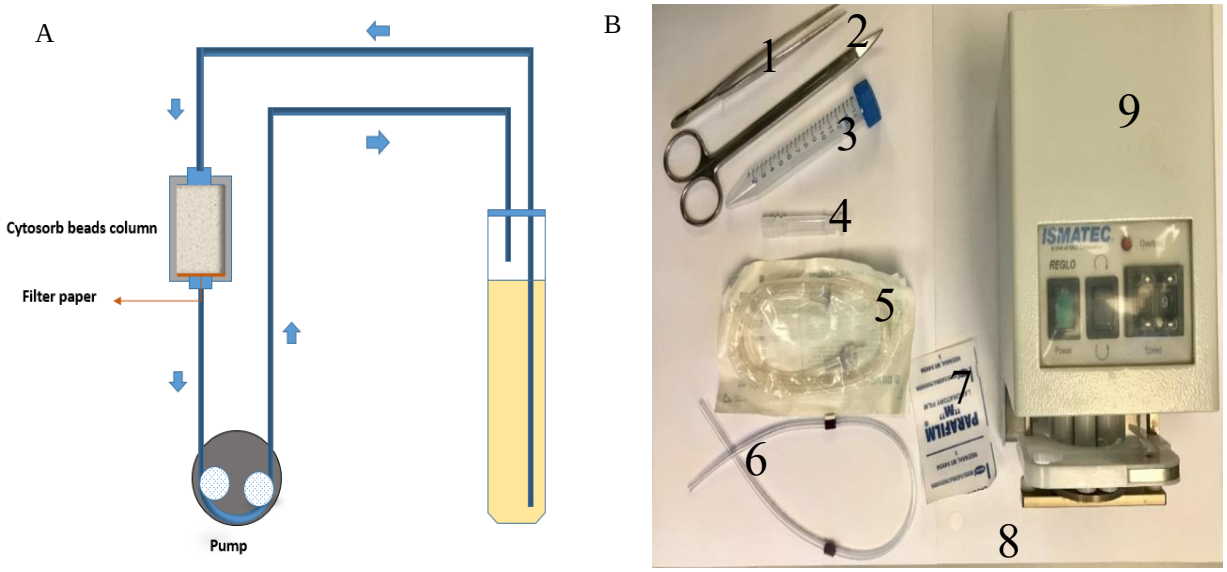

Figure 8 Diagram (A) and materials (B) applied in the mini plasma adsorption system
1. pliers, 2. scissors, 3. 15 ml tube, 4. 1 ml column tube, 5. infusion extension tube, 6. pump tubing (ID 2.06 mm), 7. parafilm, 8. filter paper, 9. pump (manufacturer's information is included in Table 6).

2.6 Statistics

Statistical analysis was performed using GraphPad Prism statistical software v6.0 (GraphPad, CA, USA). Data are presented as the means ± SEM, unless otherwise

indicated. A two-tailed paired t-test was applied for detecting differences between two groups (untreated vs. treated or SAA vs. SAA + antagonists) in nitrite production and cytokine detection experiments. Significance was accepted at $P < 0.05$.

Table 9 Principles of the enzymatic photometric assays for lipids and lipoproteins

Lipids and lipoproteins	Assay reaction	Explanation
LDL	1) LDL + reagent 1 ——> Protected LDL HDL, VLDL, Chylomicrons $\xrightarrow{\text{CHE \& CHO}}$ Cholestenone + H_2O_2 $H_2O_2 \xrightarrow{\text{Catalase}} H_2O$ 2) Protected LDL + reagent 2 ——> LDL LDL-C $\xrightarrow{\text{CHE \& CHO}}$ Cholestenone + H_2O_2 H_2O_2 + 4-Aminoantipyrine + H-DAOS $\xrightarrow{\text{POD}}$ Color	1) LDL-C is selectively protected while non-LDL-lipoproteins are enzymatically processed. 2) LDL-C is released and selectively determined.
HDL	1) LDL, VLDL, Chylomicrons $\xrightarrow{\text{Anti-human β-lipoprotein antibodies}}$ Antigen-antibody complexes + HDL 2) HDL-cholesterol + $H_2O + O_2 \xrightarrow{\text{CHE \& CHO}}$ Cholest-4-en-3-one + fatty acid + H_2O_2 H_2O_2 + F-DAOS + 4-Aminoantipyrine $\xrightarrow{\text{POD}}$ Blue complex + H_2O	1) Reagent 1 including antigen-antibody complexes with LDL, VLDL and chylomicrons can protect these lipoproteins from the enzyme. 2) HDL-C is selectively reactive to CHE and CHO in Reagent 2.
Triglycerides	Triglycerides $\xrightarrow{\text{LPL}}$ Glycerol + fatty acid Glycerol + ATP $\xrightarrow{\text{GK}}$ Glycerol-3-phosphate + ADP Glycerol-3-phosphate + $0_2 \xrightarrow{\text{GPO}}$ Dihydroxyaceton phosphate + H_2O_2 2 H_2O_2 + Aminoantipyrine + 4-Chlorophenol $\xrightarrow{\text{POD}}$ Quinoneimine + HCl + 4 H_2O	Triglycerides levels are determined after an enzymatic reaction by lipoprotein lipase. Finally, the indicator quinoneimine is generated from aminoantipyrine and 4-chlorophenol by hydrogen peroxide under the catalytic action of peroxidase. The catalysts are all included in one reagent.

Table 9 (continued)

Cholesterol	Cholesterol ester + H_2O —CHE→ Cholesterol + Fatty acid Cholesterol + O_2 —CHO→ Cholesterol-3-one + H_2O_2 2 H_2O_2 + 4-Aminoantipyrine + Phenol —POD→ Quinoneimine + 4 H_2O	Cholesterol is measured after enzymatic hydrolysis and oxidation. The colorimetric indicator is quinoneimine. Catalysts needed in this test are all included in one reagent.
Phospholipids	1) Phosphatidyl choline + H_2O —Phospholipase D→ Choline + Phosphatidic acid Choline + 2 O_2 + H_2O —Choline oxidase→ Betaine + 2 H_2O_2 2) 2 H_2O_2 + 4-Aminoantipyrine + TBHBA —Peroxidase→ Chinone dye + 4 H_2O	1) Phospholipids are tested after enzymatic hydrolysis and oxidation. 2) The colorimetric indicator is chinone dye.
Triglycerides	Triglycerides —LPL→ Glycerol + fatty acid Glycerol + ATP —GK→ Glycerol-3-phosphate + ADP Glycerol-3-phosphate + 0_2 —GPO→ Dihydroxyaceton phosphate + H_2O_2 2 H_2O_2 + Aminoantipyrine + 4-Chlorophenol —POD→ Quinoneimine + HCl + 4 H_2O	Triglycerides levels are determined after an enzymatic reaction by lipoprotein lipase. Ultimately, the indicator quinoneimine is generated from aminoantipyrine and 4-chlorophenol by hydrogen peroxide under the catalytic action of peroxidase. The catalysts are all included in one reagent.

CHE: cholesterol esterase, CHO: cholesterol oxidase, POD: 4-aminoantipyrine peroxidase, LPL: lipoprotein lipase, GK: glycerol kinase, GPO: glycerol-3-phosphate-oxidase

3 Results

3.1 IL-6, IL-1β and MCP-1 detection in THP-1 macrophages

SAA stimulates the production of proinflammatory cytokines in various cell types (Table 1) including macrophages. To assess this property, the levels of IL-6, IL-1β and MCP-1 were determined in SAA-stimulated THP-1 macrophages. The SAA-induced cytokines levels were compared to those induced by LPS, which is a class PAMP.

Both LPS and SAA could stimulate IL-6, IL-1β and MCP-1 production in THP-1 macrophages (Figure 9 A, B, C), but the cytokine levels were higher in SAA-treated cells. During the stimulation, all three cytokines were secreted in a time-response manner, especially IL-6. Since pro-IL-1β needs to be cleaved and then released from the cell, the intracellular IL-1β level was also determined and compared to the level in the supernatant, which showed that the intracellular IL-1β level was much higher than that in the supernatant, especially in SAA-stimulated cells (Figure 9 D).

3.2 TLR2 and TLR4 expression levels in THP-1 monocytes and macrophages

SAA binds to various receptors. Our team has confirmed the role of FPR2 in SAA-mediated MPC-1 generation in vascular smooth muscle cells[4]. To better understand the proinflammatory properties of SAA, two other critical receptors, TLR2 and TLR4, were included in this study. Before the stimulation experiments, the expression levels of these two receptors were quantified in THP-1 cells (macrophages and monocytes) by qRT-PCR. The TLR2 and TLR4 mRNA levels were normalized to both housekeeper genes β-actin and GAPDH. According to Figure 10 A, TLR2 and TLR4 were both expressed in THP-1 monocytes and macrophages at comparable levels. The results were confirmed by running amplified cDNA on agarose gels (Figure 10 B).

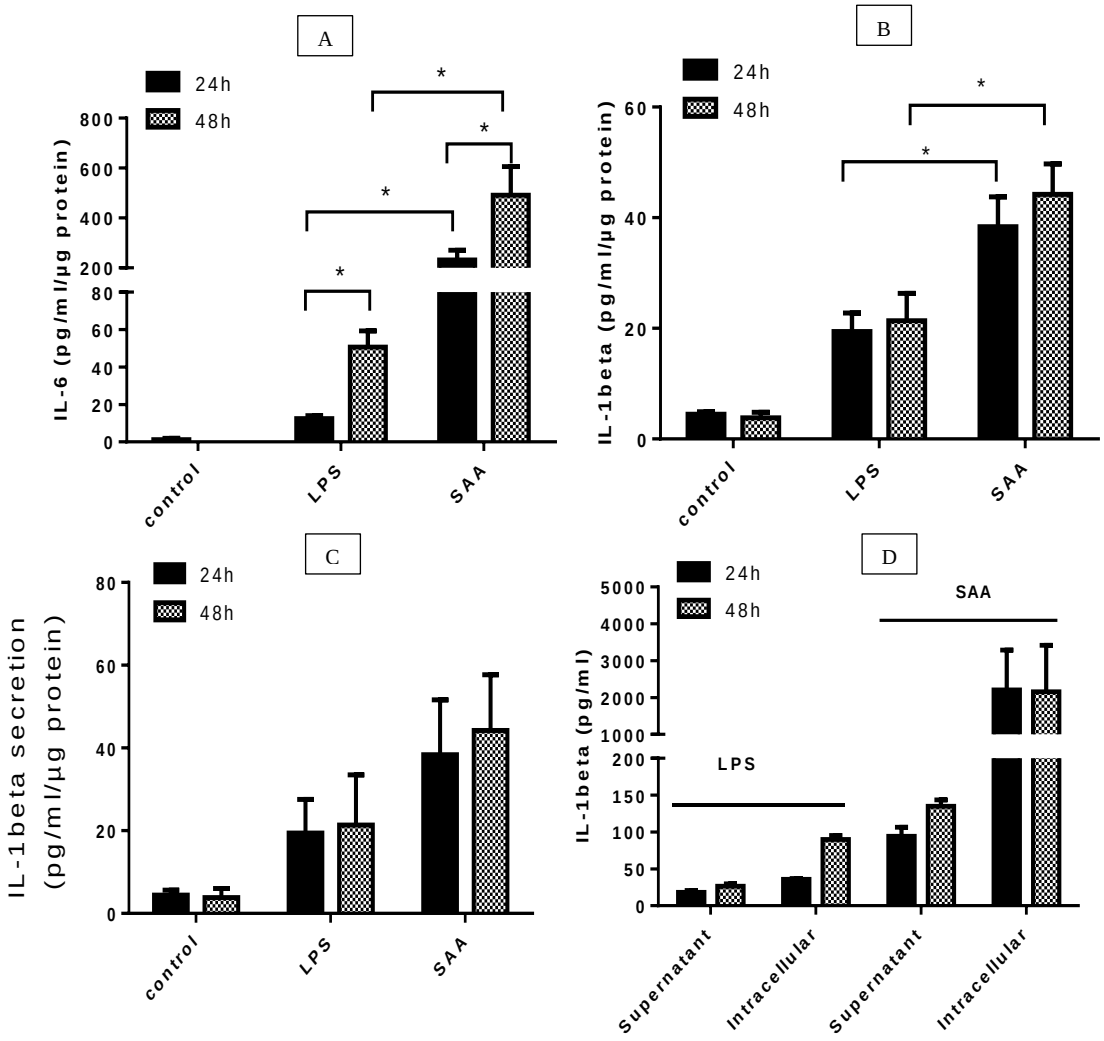

Figure 9 IL-6, IL-1β and MCP-1 detection in SAA- and LPS-stimulated THP-1 macrophages
IL-6 (A), IL-1β (B) and MCP-1 (C) were quantified in SAA- and LPS-stimulated THP-1 macrophages. Intracellular IL-1β levels in LPS- and SAA-stimulated cells were determined and compared to the levels in the supernatant (D). THP-1 macrophages were stimulated with 1 µg/ml SAA or 1 µg/ml LPS for 24 h and 48 h. No treatment in the control group. Data are presented as means ± SEM of three (IL-6 and IL-1β) or two (MCP-1) independent experiments. * $P < 0.05$ vs. control by Wilcoxon matched-pairs signed rank test.

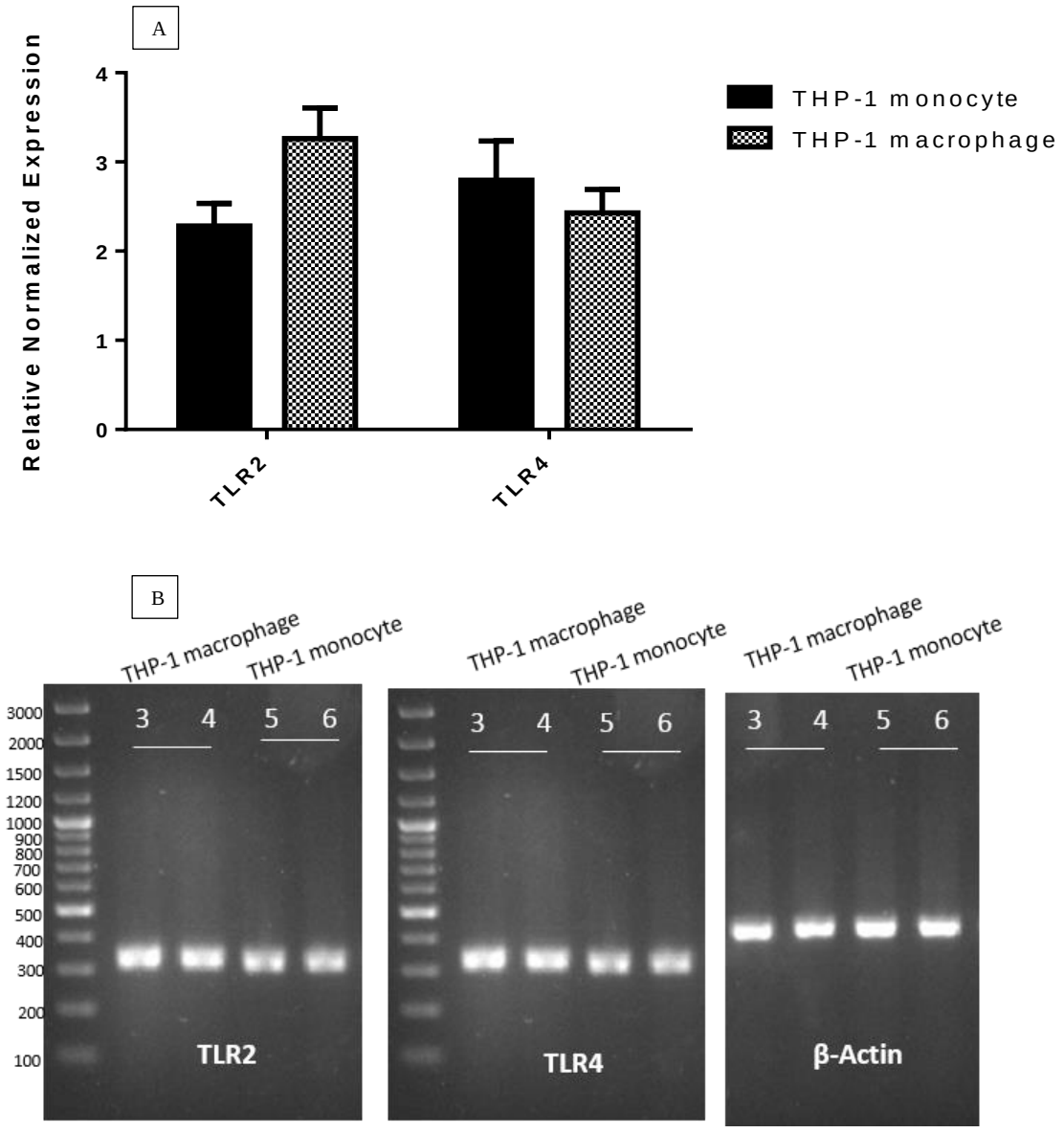

Figure 10 TLR2 and TLR4 expression levels in THP-1 monocytes and macrophages
A: The relative normalized mRNA expression of TLR2 and TLR4 in THP-1 macrophages and monocytes measured by qRT-PCR. B: Agarose gel electrophoresis of TLR2, TLR4 and β-actin PCR products, 100 bp DNA ladder. Samples 3 and 4 were from THP-1 macrophages, and samples 5 and 6 were from THP-1 monocytes. Data are presented as the means ± SEM. N ≥ 3.

3.3 The role of TLR2 and TLR4 in SAA-induced IL-6, IL-1β and MCP-1 secretion

Both the time- and dose-dependent effects of antagonists were determined to better understand the role of TLR2 and TLR4 in SAA-mediated cytokine induction. Therefore, THP-1 macrophages were stimulated by SAA or SAA + antagonists (5 μM and 10 μM) for 24 h or 48 h. The TLR4-specific antagonist TAK-242 and the TLR1/TLR2 heterodimer blocker CU CPT22 were used in this study.

The results (Figure 11) showed that TAK-242, at a concentration of 10 μM, blocked SAA-induced IL-6, IL-1β and MCP-1 in both 24 h and 48 h stimulations, while CU CPT22 only significantly inhibited MCP-1 and 24 h-induced IL-6 but had no effect on SAA-stimulated IL-1β production.

3.4 The NLRP3 inflammasome inhibitor MCC950 decreases IL-1β but has no effect on IL-6 and MCP-1 secretion in SAA-stimulated THP-1 macrophages

The NLRP3 inflammasome has been shown to be involved in a range of inflammatory conditions[100] and to participate in the process of SAA-mediated IL-1β production[48]. It has been reported that IL-1β can further induce IL-6 and MCP-1[61,101], but these cytokines may also be secreted independently[74]. It is not clear whether SAA-induced IL-1β will further promote IL-6 and MCP-1 production. To answer this question, MCC950, an inhibitor that targets NLRP3 inflammasome activation but not priming, was employed in this experiment.

THP-1 macrophages were treated with SAA and SAA plus different concentrations (0.1 μM and 1 μM) of MCC950 for 24 h and 48 h. As shown in Figure 12, MCC950 decreased SAA-induced IL-1β in 24 h and 48 h stimulation in a dose-dependent and significant manner, but did not show any inhibition of SAA-induced IL-6 and MCP-1.

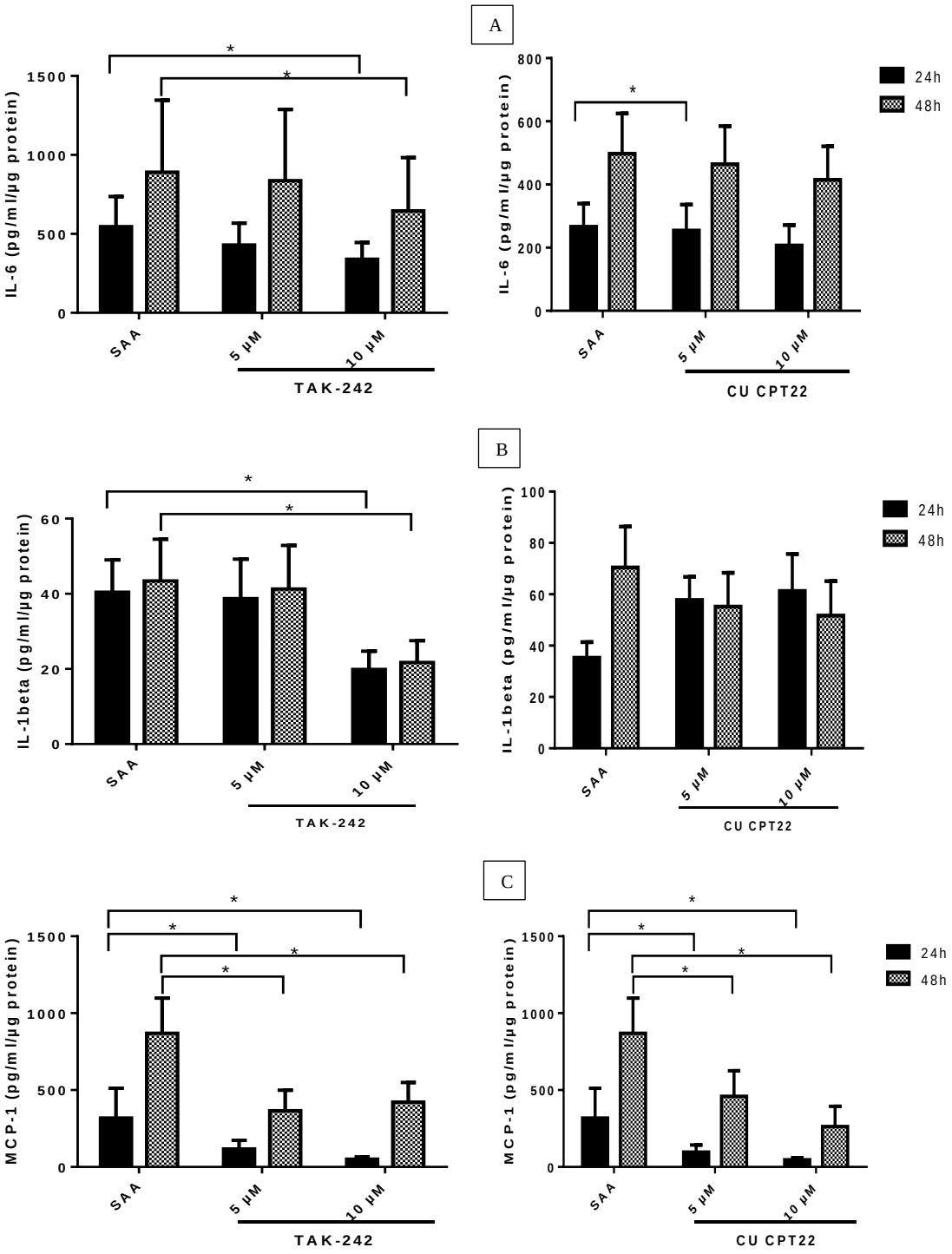

Figure 11 IL-6, IL-1β and MCP-1 detection in THP-1 macrophages co-stimulated with SAA and TAK-242, or CU CPT22

IL-6 (A), IL-1β (B) and MCP-1 (C) were quantified in THP-1 macrophages that co-stimulated with SAA and TAK-242, or CU CPT22 for 24 h and 48 h. Cells in the SAA only group were treated with SAA (10 μg/ml). Cells in different doses of TAK-242 and CU CPT22 groups were co-stimulated with 10 μg/ml SAA. Data are presented as the means ± SEM. N ≥ 3. * $P < 0.05$ vs. SAA group by Wilcoxon matched-pairs signed rank test.

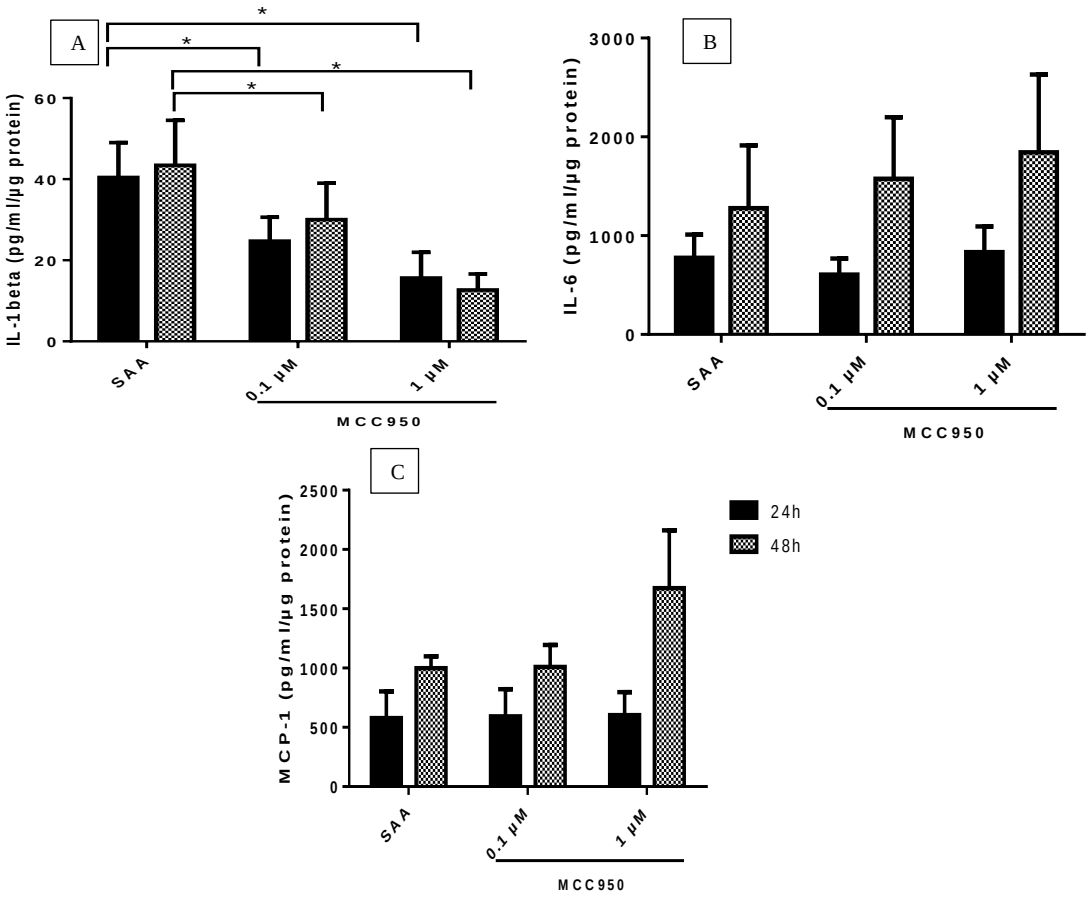

Figure 12 IL-6, IL-1β and MCP-1 detection in SAA and SAA/MCC950 co-stimulated THP-1 macrophages

IL-6 (A), IL-1β (B) and MCP-1 (C) were detected SAA and SAA/MCC950 (0.1 µM and 1 µM) co-stimulated THP-1 macrophages. Cells in the SAA group were only treated with SAA (10 µg/ml). Cells treated with different doses of MCC950 were co-stimulated with 10 µg/ml SAA. Data are presented as the means ± SEM. N ≥ 3. * P < 0.05 vs. the SAA group by Wilcoxon matched-pairs signed rank test.

3.5 Cell viability evaluation

To exclude the effects on cell toxicity of antagonists used in this project. The toxic effects of CU CPT22, TAK-242 and MCC950 on THP-1 macrophages were tested. The proliferation assay was performed for a cytotoxicity screening. This assay detects cell metabolic activity rather than directly evaluating the drug's cell toxicity. Thus, a cytotoxicity assay that determines the number of dead cells was also employed.

THP-1 macrophages were stimulated with different concentrations (0.01 µM, 0.1 µM, 1 µM, 10 µM, and 100 µM) of CU CPT22, TAK-242 and MCC950 plus 10 µg/ml SAA for 24 h and 48 h. The results of the cell proliferation assay and the cytotoxicity assay measuring cell viability were adjusted to the control group results. When co-stimulated with 10 µg/ml SAA, both CU CPT22 and TAK-242 showed significant cell toxicity for THP-1 macrophages at concentration 100 µM, the cell viability was much lower than control or other treatment groups. At concentration 10 µM or lower, both CU CPT22 and TAK-242 had no apparent cell toxicity on THP-1 macrophages, the cell viability was from 80% to 100% (Table 10 and Table 11).

In all MCC950 stimulations (also co-stimulated with 10 µg/ml SAA), the cell viability from both assays was higher than 90% after adjusted to the control group. Which means that MCC950 had no significant cell toxicity on THP-1 macrophages even at a concentration of 100 µM (Table 12). The concentrations of each antagonist in bold type in the following tables were applied in this study.

Table 10 CU CPT22 cell viability evaluation

CU CPT22 (µM)	SAA (µg/ml)	Proliferation assay		Cytotoxicity assay			
		24 h	48 h	24 h		48 h	
		Cell viability	Cell viability	Cell viability	Dead cell	Cell viability	Dead cell
0	0	100%	100%	100%	9%	100%	12%
0.01	10	102%	105%	95%	14%	81%	29%
0.1	10	102%	115%	91%	17%	85%	26%
1	10	100%	122%	91%	17%	83%	27%
10	**10**	**87%**	**90%**	**93%**	**15%**	**90%**	**21%**
100	10	80%	85%	51%	54%	65%	43%

Table 11 TAK-242 cell viability evaluation

TAK-242 (µM)	SAA (µg/ml)	Proliferation assay		Cytotoxicity assay			
		24 h	48 h	24 h		48 h	
		Cell viability	Cell viability	Cell viability	Dead cell	Cell viability	Dead cell
0	0	100%	100%	100%	9%	100%	12%
0.01	10	92%	109%	90%	18%	81%	29%
0.1	10	98%	97%	86%	21%	82%	28%
1	10	105%	137%	89%	19%	84%	26%
10	**10**	**91%**	**134%**	**90%**	**19%**	**93%**	**19%**
100	10	65%	64%	76%	31%	27%	76%

Table 12 MCC950 cell viability evaluation

MCC950 (μM)	SAA (μg/ml)	Proliferation assay		Cytotoxicity assay			
		24 h	48 h	24 h		48 h	
		Cell viability	Cell viability	Cell viability	Dead cell	Cell viability	Dead cell
0	0	100%	100%	100%	7%	100%	7%
0.01	10	152%	175%	97%	9%	95%	11%
0.1	**10**	**146%**	**171%**	**98%**	**10%**	**96%**	**11%**
1	**10**	**149%**	**185%**	**98%**	**9%**	**95%**	**12%**
10	10	152%	173%	97%	10%	95%	12%
100	10	103%	109%	97%	12%	92%	15%

3.6 Nitrite production detection

NO is a free radical and a critical cell signaling molecule that plays an essential role in diverse pathophysiological processes such as the endothelial dysfunction[102], macrophage proliferation[103] and immune responses[82]. Therefore, this section aims to investigate the ability of SAA to induce NO production and the pathway involved in this process. Nitrite production levels were first quantified in SAA- and LPS-stimulated RAW 264.7 cells and THP-1 cells. However, no production was detected in THP-1 monocytes and macrophages (data not shown). Therefore, only RAW 264.7 cells were employed in the signaling pathway detection.

3.6.1 Nitrite production detection in SAA- and LPS-stimulated RAW 264.7 cells

RAW 264.7 cells were treated with different concentrations (0.1 μg/ml, 1 μg/ml and 10 μg/ml) of LPS and SAA. After a 24 h stimulation, a dose-response increase in nitrite production was found in SAA- and LPS-treated RAW 264.7 cells (Figure 13 A). Results were from one stimulation and no statistical significance was found between the control and LPS- or SAA-treated cells. When compared results from 6 stimulations, 1 μg/ml LPS or 10 μg/ml SAA promoted significantly increased nitrite production in RAW 264.7 cells (Figure 13 B).

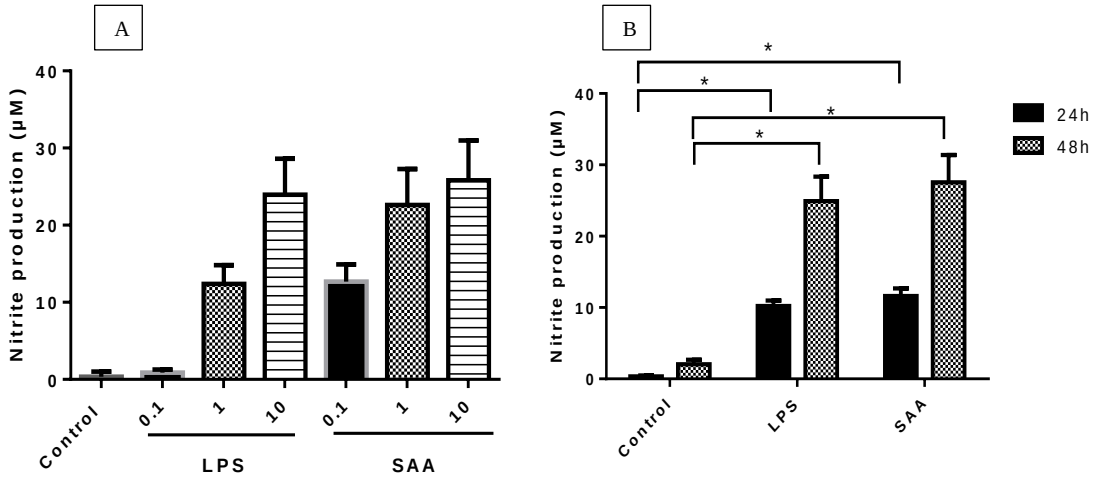

Figure 13 Nitrite production detection in SAA- and LPS-stimulated RAW 264.7 cells
A: RAW 264.7 cells were stimulated with different concentrations (0.1 μg/ml, 1 μg/ml and 10 μg/ml) of LPS and SAA for 24 h. A dose-response increase in nitrite production was found in SAA- and LPS-treated RAW 264.7 cells. No treatment in the control group. Data are presented as the means ± SEM of triplicated wells. LPS and SAA groups were compared to control group. No statistical significance was found. B: RAW 264.7 cells were stimulated with 1 μg/ml LPS or 10 μg/ml SAA for 24h and 48h. Data are presented as the means ± SEM. N ≥ 3. * P < 0.05 vs. the control group by Wilcoxon matched-pairs signed rank test.

3.6.2 The role of TLR2, TLR4 and NLRP3 in SAA-stimulated nitrite production in RAW 264.7 cells

According to previous studies, TLRs play essential roles in NO upregulation[104,105]. Therefore, the role TLR2 and TLR4 in SAA-induced NO production was determined in this section. After 24 h and 48 h stimulation, both TLR2 and TLR4 antagonists of significantly inhibited of SAA-induced nitrite production in RAW 264.7 cells (Figure 14).

In addition to TLR activation, cytokines such as IL-1β can also trigger iNOS gene transcription[106]. Therefore, the NLRP3 inflammasome pathway was also tested here. As shown in the previous section, 1 μM MCC950 remarkably decreased SAA-induced IL-1β levels (Figure 12), but this inhibitor did not show any effect on the SAA-stimulated nitrite production (Figure 14).

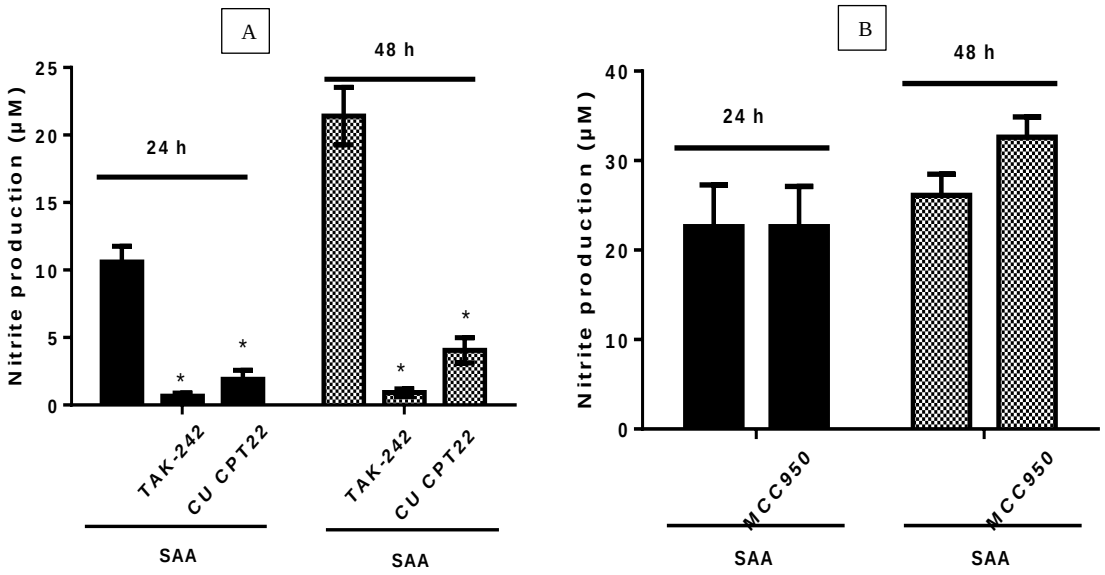

Figure 14 Nitrite production measurement in RAW 264.7 cells co-stimulated with SAA and TAK-242, CU CPT22, or MCC950

Nitrite production was detected in RAW 264.7 cells that stimulated with SAA (1 μg/ml) with or without TAK-242 (10 μM) or CU CPT22 (10 μM) (A) or MCC950 (1 μM) (B) for 24 h and 48 h. Data are presented as the means ± SEM of 3 independent experiments. Co-stimulated groups were compared with the SAA-stimulated group. * $P < 0.05$ by Wilcoxon matched-pairs signed rank test.

3.7 ROS detection

ROS are a group of reactive chemical molecules that can be toxic to the cell and contribute to the pathological processes of atherosclerosis[76]. Furthermore, ROS participate in multiple cell signaling pathways[78] such as NLRP3 activation[79]. ROS are generated from two major sites in the cell and can be classified as intracellular ROS and mitochondrial ROS. These ROS might play distinct roles during cell signaling pathway activation. Therefore, both mitochondrial-derived ROS and intracellular generated ROS were detected in RAW 264.7 cells and THP-1 cells after the LPS and SAA stimulation.

3.7.1 SAA promotes intracellular ROS in monocytes and macrophages

Intracellular ROS were detected at 2 h, 4 h, 8 h, and 24 h treatment time points. The ROS level in SAA- or LPS-treated myeloid cells peaked at 2 h to 8 h and decreased afterward. Thus, Figure 15 only shows the ROS level in the early stimulation time points. At the same concentration, the ROS levels were higher in SAA-treated cells than LPS-treated control cells. No statistical significance was detected, which might be due to the limited number of test samples.

3.7.2 SAA promotes mitochondrial ROS production in RAW 264.7 cells

At the 2 h, 4 h, 8 h, and 24 h treatment time points, no mitochondrial ROS was detected in SAA- or LPS-treated THP-1 cells (data not shown), while mitochondrial ROS increased in both SAA- and LPS-treated RAW 264.7 cells after 24 h (Figure 16). The 24 h stimulated mitochondrial ROS also seemed higher in the SAA group when compared to the LPS group.

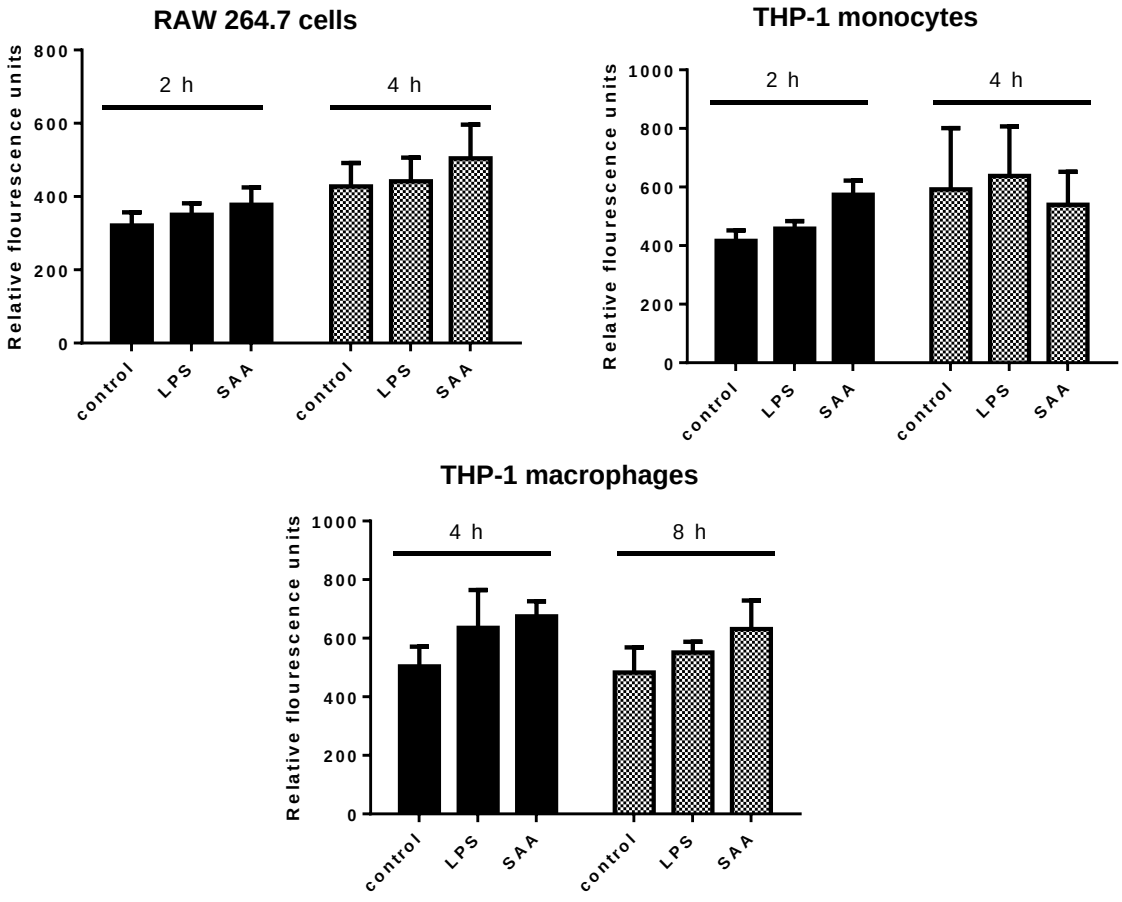

Figure 15 Intracellular ROS detection in LPS- and SAA-stimulated cells
RAW 264.7 cells, THP-1 monocytes and THP-1 macrophages were treated with 1 µg/ml SAA or 1 µg/ml LPS. No treatment of cells in the control group. N ≥ 3. Data are presented as the means ± SEM of fluorescence values.

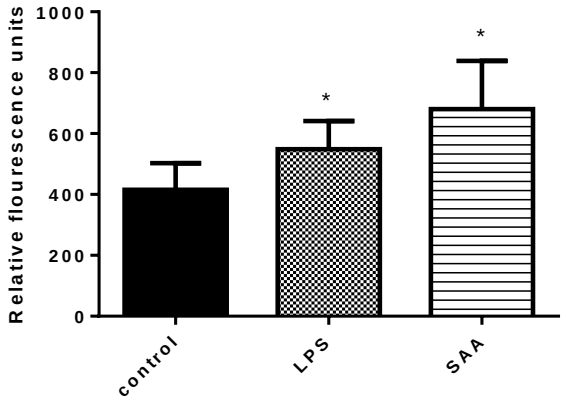

Figure 16 Mitochondrial ROS detection in LPS- or SAA-stimulated RAW 264.7 cells
RAW 264.7 cells were treated with 1 µg/ml SAA or 1 µg/ml LPS for 24 h. No treatment of cells in the control group. N ≥ 3. Data are presented as the means ± SEM of fluorescence values. * P < 0.05 vs. the control by Wilcoxon matched-pairs signed rank test.

3.8 Experimental setting for SAA adsorption

The previous sections verified the proinflammatory properties of SAA. These properties partially explain the association found between elevated SAA and complications in CKD patients. Regular renal replacement treatment can barely remove SAA. Therefore, the purpose of this section is to explore methods to remove SAA from the circulation. A mini plasma adsorption system was established to evaluate the adsorption of CytoSorb™ adsorber and another novel material. The procedure is shown in the Methods section in Figure 8. During the blood purification, one problem is that some “good” substances such as albumin will be lost as well. To test the adsorption of those materials, protein, triglycerides, total cholesterol, phospholipids, HDL-C, LDL-C and CRP were also detected.

3.8.1 Nonspecific binding test

To exclude the nonspecific binding, the system without adsorbent beads was tested first. Samples were run in the system without beads for 72 h, and substances were measured in the samples before and after the procedure. The results in Table 13 show that after the 72 h, no apparent adsorption of the tested substances by this system (without adsorbent beads) was found.

Table 13 System adsorption test

	Serum + SAA Average ± SD (reduced concentration)	N	Serum Average ± SD (reduced concentration)	N
SAA concentration (µg/ml)	-6.83 ± 11.92	2	-0.10 ± 0.69	2
Protein (mg/ml)	-3.60 ± 0.14	2	-0.91 ± 3.59	2
HDL-C[mg/dl]	11.24 ± 10.75	2	4.88 ± 1.45	2
LDL-C [mg/dl]	5.71 ± 7.44	2	21.38	1
Triglycerides [mg/dl]	-8.10 ± 20.55	2	-4.06 ± 1.29	2
Cholesterol [mg/dl]	-2.38 ± 6.14	2	-0.83 ± 7.57	2
Phospholipids [mg/dl]	-2.83 ± 16.28	2	8.49 ± 2.72	2
CRP concentration (µg/ml)	0.15	1	-0.79	1

Note: Samples were divided into two equal portions, which were mixed with or without additional SAA. The samples were run in the system without adsorbent bead for 72 h. Data are presented as the means ± SD of the reduced concentration after 72 h of running two independent tests. SAA, serum amyloid A; HDL-C, high-density-lipoprotein cholesterol; LDL-C, low density lipoprotein cholesterol; CRP, C-reactive protein.

3.8.2 CytoSorb™ adsorber evaluation

CytoSorb™ adsorber are biocompatible beads designed to remove pro- and anti-inflammatory mediators between a molecular weight of 5-60 kDa. In previous studies, CytoSorb™ adsorber has shown a good ability to reduce cytokines[97,98]. However, there are no available data on CytoSorb™ adsorber removing SAA.

To test the SAA adsorption, 20 ml serum was divided into two equal portions. A total of 31.25 µg/ml recombined human SAA was added to one tube with 10 ml serum, which is the “serum + SAA” group in the following figures. Another tube with 10 ml serum without additional SAA is the “serum” group. Serum from both tubes was run in the mini plasma adsorption system simultaneously. Samples were collected after running for 0 h, 4 h, 24 h, 48 h and 72 h. Bead columns were replaced by new columns every 24 h. SAA, total protein, triglycerides, total cholesterol, phospholipids, HDL-C, LDL-C and CRP were determined in those samples. According to the results shown in the following figures, both recombinant SAA and natural SAA can be removed by CytoSorb™ adsorber (Figure 17). This adsorber also eliminates proteins, cholesterols and lipids. After 72 h treatment, most of these substances were removed from the serum (Figure 17, Figure 18, Figure 19).

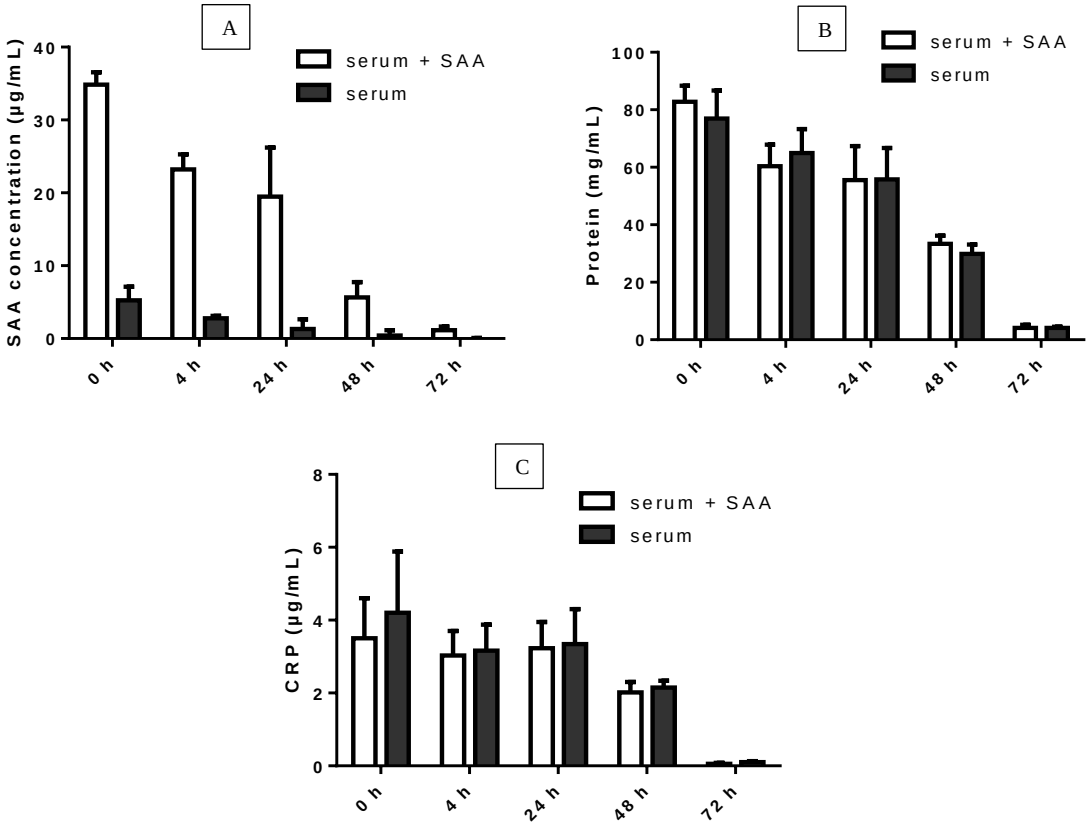

Figure 17 SAA, protein and CRP adsorption by Cytosorb™ adsorber
SAA (A), protein (B) and CRP (C) levels during Cytosorb™ adsorber treatment. A total of 31.25 µg/ml SAA was added to the serum in the serum + SAA group. Samples were collected after running them in the system for 0 h, 4 h, 24 h, 48 h, and 72 h. Bead columns were replaced by new ones every 24 h. Data are presented as the means ± SD of 3 independent experiments.

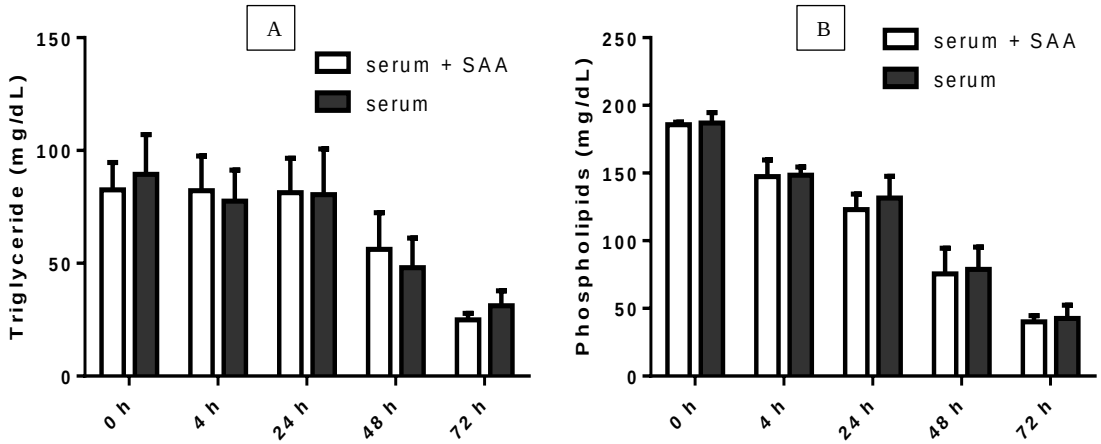

Figure 18 Lipids adsorption by Cytosorb™ adsorber
Triglycerides (A) and phospholipids (B) levels during Cytosorb™ adsorber treatment. A total of 31.25 µg/ml SAA was added to the serum in the serum + SAA group. Samples were collected after running them in the system for 0 h, 4 h, 24 h, 48 h, and 72 h. Bead columns were replaced by new ones every 24 h. Data are presented as the means ± SD of 3 independent experiments.

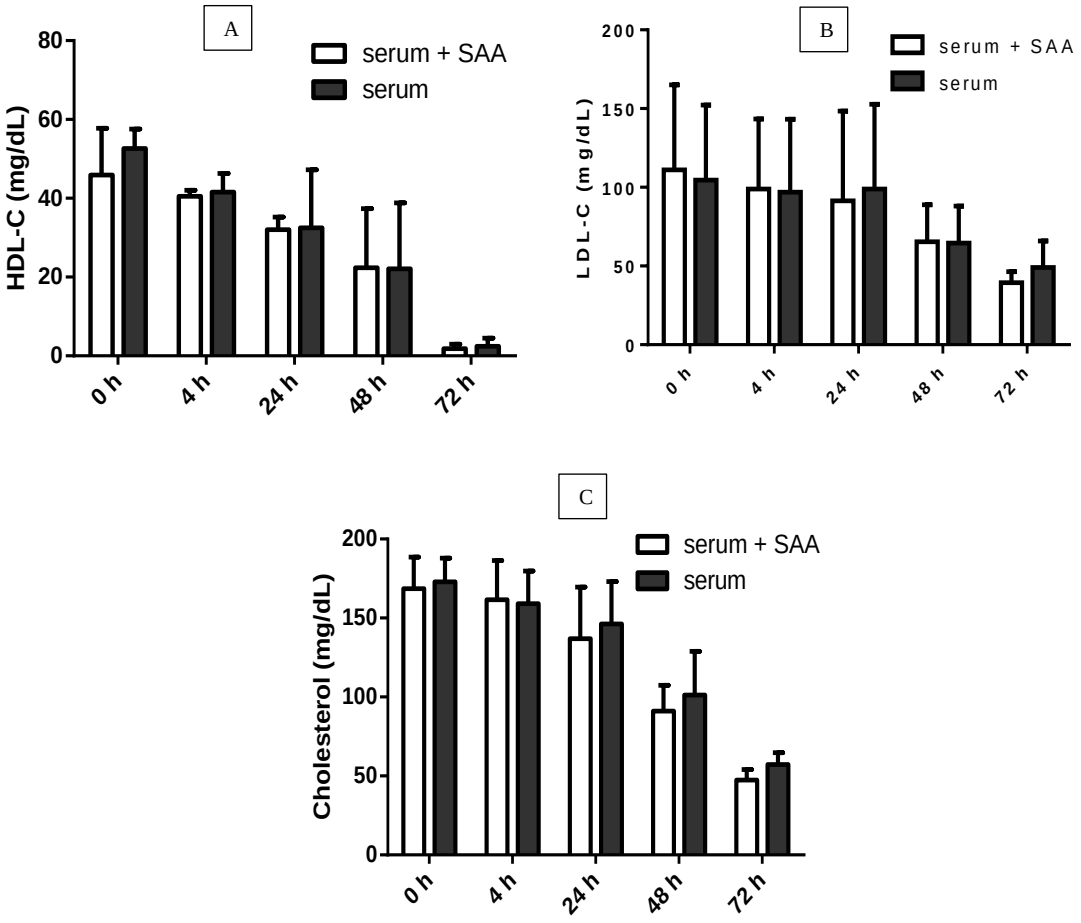

Figure 19 Cholesterol adsorption by Cytosorb™ adsorber
HDL-C (A), LDL-C (B) and total cholesterol (C) levels during Cytosorb™ adsorber treatment. A total of 31.25 µg/ml SAA was added to the serum in the serum + SAA group. Samples were collected after running them in the system for 0 h, 4 h, 24 h, 48 h, and 72 h. Bead columns were replaced by new ones every 24 h. Data are presented as the means ± SD of 3 independent

3.9 Summary of results

- SAA can induce IL-6, IL-1β and MCP-1 in THP-1 macrophages.
- TLR4 participates in SAA-mediated IL-6, IL-1β and MCP-1 production in THP-1 macrophages.
- TLR2 plays a role in the SAA-induced upregulation of MCP-1 and IL-6 but is not involved in SAA-induced IL-1β secretion.
- SAA induces IL-1β through the NLRP3 inflammasome.
- The SAA-promoted IL-6 and MCP-1 generation is not dependent on the NLRP3 inflammasome.

- SAA can trigger nitrite production in RAW 264.7 cells but not in THP-1 cells.
- Both TLR2 and TLR4 are involved in SAA-induced nitrite production in RAW 264.7 cells.
- The SAA-induced nitrite production is NLRP3 inflammasome independent.
- SAA upregulates intracellular and mitochondrial ROS in myeloid cells.
- CytoSorb^{TM} adsorber can remove SAA from plasma.

4 Discussion

SAA was initially recognized as a biomarker for rheumatic diseases[107]. At the same time, this protein was found to be associated with HDL and was named apoSAA[108]. During the first decades, similar to CRP, SAA was only considered an acute phase reaction protein and a biomarker for inflammatory diseases. However, more evidence in the subsequent studies indicated that SAA is an immunologically active protein. For instance, SAA can induce the production of numerous cytokines via distinct receptors in different cells (Table 1) including macrophages. Since macrophages play a fundamental role in atherosclerosis, the SAA-mediated cytokine production in this cell type might be a remarkable reason for the development of this disease. Therefore, the first part of this study investigated the signaling pathway for SAA promoting the production of inflammatory mediators in macrophages, especially IL-1β, IL-6, MCP-1, nitrite production and ROS. Moreover, our previous work demonstrated increased SAA levels in CKD patients from dialysis units, which suggests a low efficiency of SAA removal by regular dialysis[4]. The proinflammatory property of SAA combined with this elevated level provide an explanation for the association found between SAA levels and cardiovascular complications in CKD patients. Accordingly, this study also explored methods for removing SAA from the bloodstream.

4.1 Proinflammatory cytokines from SAA-stimulated macrophages

Similar to previous reports, a significant increase in IL-1β, IL-6 and MCP-1 was detected in SAA-stimulated cells, which verified the cytokine-inducing property of SAA in human macrophages.

An interesting finding in this study is that the recombinant SAA used in this study mediates higher levels of IL-1β, IL-6 and MCP-1 secretion when compared to LPS. Two major reasons might be responsible for this outcome. First, LPS is a TLR4-specific agonist, whereas SAA is a ligand for multiple receptors (Table 1). The simultaneous activation of several receptors might lead to higher levels of cytokines. Another probable cause is the recombinant SAA that is a hybrid between human SAA1α and SAA2β used in this study. It has been reported that

this SAA has a more potent capability of inducing cytokines compared to the purified natural SAA[109]. The proinflammatory properties of purified HDL-disassociated and HDL-associated SAA has been demonstrated by our lab and other research teams as well[4-6]. Moreover, the concentration (1 μg/ml) of LPS applied in this study was even higher than the level in sepsis patients (approximately 0.5 μg/ml)[110], while the concentration of SAA (1 μg/ml) used in this study was much lower than that in sepsis patients (up to 1 mg/ml). This concentration is also below the level in CKD patients (approximately 10-30 μg/ml). All these results suggest that the sustained elevated SAA in patients is an inflammatory mediator rather than just an acute phase reaction protein.

Another observation that needs to be discussed here is that SAA cannot efficiently induce the release of IL-1β from THP-1 macrophages. Less than 1/10 of intracellular IL-1β was released into the supernatant in SAA-stimulated cells. According to previous studies, unlike LPS, which only upregulates pro-IL-1β but cannot induce the release of the mature cytokine[111], SAA can independently promote IL-1β release[48,68]. In this study, the supernatant/intracellular IL-1β ratio was even lower in SAA-treated cells when compared to LPS-stimulated cells. This means that, SAA cannot readily promote the release of IL-1β. The activation of the NLRP3 inflammasome plays a central role in IL-1β maturation. The issue regarding activators for NLRP3 will be discussed in the next section.

4.2 SAA-induced IL-1β is TLR4- and NLRP3 inflammasome-dependent

This study found that SAA promotes IL-1β release through TLR4 in human macrophages. However, in both HeLa cells[112] and mouse macrophages[113], TLR2 rather than TLR4 mediates SAA-mediated release of IL-1β. In keratinocytes, antibodies for TLR2 and TLR4 both downregulate IL-1β expression[48]. Our results have shown that the expression levels of TLR2 and TLR4 are comparable in THP-1 macrophages, which excludes the possibility that the low expression of TLR2 may lead to the negative finding in TLR2 antagonist treatment. Diverse cell types and experimental designs could cause the disparity between ours and others

results. Since data from identical experimental settings are not available, our results need to be confirmed in future investigations.

It has been reported that SAA stimulates IL-1β secretion via NLRP3 inflammasome-caspase-1[49,68]. MCC950 also blocks SAA-induced IL-1β in this study. MCC950 is a highly specific inhibitor of both canonical and noncanonical activation of the NLRP3 inflammasome[114]. The mechanism for this blockade is still not clear. Until now, we only knew that MCC950 neither suppresses NLRP3 priming nor interrupts the NLRP3 and ASC interaction but targets NLRP3 directly[114]. With a concentration of 1 μM, MCC950 nearly entirely abrogates the LPS-induced IL-1β[114,115], but this inhibitor only partially blocks SAA-induced IL-1β in our experiments. One possible reason for this discrepancy is that alternative signaling pathways might exist for SAA mediating IL-1β maturation. IL-1β can be processed through an NLRP3 inflammasome-independent way[67]. For instance, an enzyme called proteinase 3 can also facilitate IL-1β maturation[116]. Another possible cause is the pro-IL-1β was released into the supernatant. The antibody used in Luminex™ assay cannot differentiate between pro-IL-1β and mature IL-1β. A certain percentage of the detected IL-1β in the supernatant might be pro-IL-1β. Other measurements, such as Western blotting, may help to further interpret this issue. On the other hand, MCC950 still blocks major SAA-induced IL-1β. Since the NLRP3 inflammasome needs to be activated to process IL-1β secretion, the activators should be present in SAA-stimulated cells. An ATP gated receptor, $P2X_7$, has been found to be involved in SAA-mediated NLRP3 inflammasome activation[49]. However, this study did not find any ATP released from cells after SAA stimulation[49]. Intracellular IL-1β (pro-IL-1β) was not determined in previous studies[48,68]. The mechanism of SAA-induced NLRP3 inflammasome activation is still unknown. In patients with elevated SAA such as CKD patients, activators of the NLRP3 inflammasome can be frequently found, e.g., electrolyte imbalance and increased ROS. These activators are very likely to release SAA-upregulated intracellular IL-1β.

4.3 SAA promotes IL-6 generation through TLR2 and TLR4, but in an NLRP3 inflammasome-independent way

This study shows that SAA mediates IL-6 generation in human macrophages through TLR2 and TLR4, whereas a TLR4 antagonist seemed more efficient at suppressing SAA-induced IL-6. Both TLR2 and TLR4 have been found to mediate SAA-induced IL-6[36,44,51,52]. Moreover, other SAA receptors, SR-BI, RAGE and FPR2, have also been investigated, but these receptors did not mediate SAA-induced IL-6 secretion in human primary chondrocytes[51].

In addition to TLRs ligands, other mediators such as IL-1β, TNF-α, ROS, and prostaglandins, can also promote IL-6 gene transcription[117]. In an earlier study, an IL-1β-deficient mouse model showed reduced IL-6 production[61], which suggested a role for IL-1β in IL-6 generation. Signaling pathway studies have revealed that IL-1β mediates IL-6 generation through MAPK, AP-1 and NF-κB[118,119]. MCC950 also suppressed IL-6 production in studies *in vivo* and *in vitro*[114,115]. Our results show that MCC950 has no effect on SAA regulation of IL-6. One possible reason for this is the relatively low IL-1β concentration in supernatants. Both SAA and IL-1β can mediate IL-6 production via NF-κB. In this case, the IL-6 gene might have already been fully induced by SAA, and the subsequently released IL-1β could have no or few effects on IL-6 induction. The high intracellular IL-1β level and the comparable released IL-6 level both indicate a compelling case for SAA-mediated NF-κB activation. These results suggest that SAA itself can effectively promote IL-6 secretion via TLR2 and TLR4. SAA-induced IL-1β does not contribute much to IL-6 generation.

4.4 TLR2 and TLR4 play more critical roles in the early stage of MCP-1 secretion in SAA-stimulated macrophages

In this study, at a concentration of 10 μM, antagonists for TLR2 and TLR4 both reduced the SAA-induced MCP-1 to approximately 10% after 24 h of costimulation. However, this inhibition diminished after 48 h of costimulation, which only reduced SAA-induced MCP-1 to 50%. The diminished effects at the 48 h costimulation indicate a more critical role of TLR2 and TLR4 in the early stage of SAA-promoted

MCP-1 production. Other receptors might be involved in the later phase. Part of the results of this section have been published. The role of TLR2 and TLR4 in SAA-mediated MCP-1 production has been confirmed in knockout mice in our lab[120]. Apart from monocyte recruitment, MCP-1 can facilitate oxLDL uptake by macrophages and promote the formation of foam cells[121,122]. The activation of TLRs in macrophages also results in oxLDL-induced foam cell formation and plaque instability[123]. SAA might be a junction between those events, i.e., SAA mediates MCP-1 production via TLR2 and TLR4 in macrophages, which promotes oxLDL uptake and foam cell formation, and finally initiates atherosclerosis. Another two receptors have also been investigated in our lab, and the results have demonstrated that FPR2 is involved in SAA-induced MCP-1 in VSMCs[4], while the $P2X_7$ antagonist dose not suppress MCP-1 in SAA-stimulated cells[120].

The NLRP3 inflammasome pathway was also tested in this study, and MCC950 had no effect on SAA-induced MCP-1 production. After the activation of TLR2 and TLR4 by SAA, the intracellular signaling pathway including IκBα and subsequently NF-κB is activated and mediates MCP-1 production[120]. IL-1β has also stimulate MCP-1 gene transcription via NF-κB[72]. A reduction in MCP-1 has also been found in MCC950-treated mice[124]. The inability of MCC950 to inhibit MCP-1 production in this study might be based on low IL-1β levels and short-term stimulation. These results should be further evaluated in experiments with extended stimulation of SAA plus NLRP3 inflammasome activators.

4.5 SAA induces nitrite production in murine macrophages via TLR2 and TLR4

In addition to proinflammatory cytokines, SAA also triggers nitrite production in murine macrophages in this research study, which has also been shown in a previous study[90], however no increased NO was detected in THP-1 monocytes and macrophages. Unlike the high level of iNOS expression in LPS-stimulated murine macrophages, LPS dose not upregulate iNOS expression in human macrophages due to the heavily methylated promoter of the human iNOS gene[125]. Therefore, most scientists have employed murine macrophages in their research.

However, in a recent study, a relatively low level of iNOS was detected in human M2 macrophages[83]. Overall, the results of inducible NO research from murine experiments should be cautiously interpreted and verified. The outcome from the SAA-triggered NO production needs to be explored by additional experiments, such as *in vivo* studies.

TLR2 and TLR4 are two functional receptors for SAA that trigger nitrite production in macrophages according to our results. Both cell membrane-expressed TLRs (TLR2, 4, 5) and endosomal membrane-expressed TLRs (TLR3, 7, 8, 9) have been demonstrated to mediate signaling transduction that upregulates iNOS[104]. The iNOS promoter contains NF-κB-binding elements that can be stimulated by TLR ligands[126]. Other activators of iNOS gene expression include IL-1β, IFN-γ and TNF-α[106]. The activation of TLR2 and TLR4 can either directly induce iNOS gene transcription or indirectly trigger further NO production after promoting cytokine secretion. The results described in a previous section have demonstrated that SAA mediates IL-1β production in macrophages via the NLRP3 inflammasome, but the blockade of this inflammasome did not reduce SAA-triggered nitrite production. With the significant reduction in NO production by TLR2/TLR4 antagonists, which was even more obvious after a 48 h costimulation, we can conclude that SAA triggers nitrite production in a direct way via TLR2 and TLR4 rather than through SAA-induced cytokines. In murine macrophages, only TLR4 but not TLR2 has been identified as a receptor for SAA-induced NO production[50,105]. The SAA-TLR2-NO signaling pathway needs to be further confirmed.

4.6 SAA promotes ROS generation in myeloid cells

Due to the upregulated antioxidant systems in THP-1 cells and cultured macrophages, the ROS levels in LPS-stimulated THP-1 cells and RAW 264.7 cells are much lower than the levels in primary cells with the same stimulation[127]. However, in this study, during the early stage (2-8 h) of stimulation, the SAA-treated cells (RAW 264.7 cells, THP-1 monocytes and THP-1 macrophages) generated more intracellular ROS than the control cells. Mitochondrial-derived ROS were only detected in RAW 264.7 cells after a 24 h stimulation. One previous

study has also found intracellular ROS and mitochondrial-derived ROS in SAA-treated mouse peritoneal macrophages[69]. However, intracellular ROS in this study were only found at the 24 h treatment, and mitochondrial ROS were detected at the 2 h stimulation[69]. These time points are far apart from those in our research. SAA-stimulated early ROS generation (within minutes) has also been found in fibroblasts[80]. Since ROS are a group of reactive chemical molecules, different fluorescent probes applied in those studies might lead to distinct results.

ROS-induced oxidative stress also contributes to the development of atherosclerosis[76]. On the other hand, the participation of ROS in multiple cell signaling pathways and the consequent proinflammatory cytokine generation could also promote the development of this disease[78]. This ROS-upregulation property of SAA might partly explain the association found between elevated SAA and the increased risk of cardiovascular diseases. Since SAA-triggered ROS are temporary rather than continuously increased, they are thought to play a more critical role in cell signaling transmission.

4.7 Reduction of SAA by CytoSorb™ adsorber

Several case reports have verified the effect of CytoSorb™ adsorber in patients with severe systemic inflammatory response syndrome (SIRS)[128-131]. Conditions in those patients include post-liver transplantation, post-cardiopulmonary bypass, acute respiratory distress syndrome (ARDS) and postcardiac surgery[128-131]. CytoSorb™ therapy has shown benefits for SIRS patients. The reduction in proinflammatory cytokines (e.g., IL-6, IL-8 and MCP-1) was in parallel with the improvement of clinical findings during the treatment. Moreover, CytoSorb™ adsorber showed a good ability to reduce bilirubin, which has a neural toxicity in its unconjugated status[128,131], while in another randomized controlled clinical trial, which enrolled 37 post-cardiopulmonary bypass (CPB) patients, no difference in the IL-6 and CRP levels was found between the control group and the CytoSorb™ adsorber-treated group[132]. Distinct patient conditions might lead to heterogeneous results. Compared to CPB surgery patients, patients with SIRS had a much higher level of the tested cytokines. For instance, the concentration of IL-6 was up to

20,000 pg/ml in ARDS-associated SIRS patients while the average peak concentration of IL-6 was 20 pg/ml in those post-CPB patients[130].

To our knowledge, this is the first study to investigate methods to remove SAA from human blood. CytoSorb™ adsorber is consists of biocompatible beads designed to capture and adsorb substances by size exclusion and nonselective hydrophobic interaction. Normally, mediators between a 5-60 kDa molecular weight can be adsorbed by these beads. However, after associating with HDL in the circulation, the molecular weight of SAA-HDL is more than 300 kDa, which might result in the low clearance rate of SAA in patients receiving regular dialysis treatment. In this study, CytoSorb™ adsorber showed a good ability to remove SAA from plasma, regardless of the use of recombinant or natural SAA. The SAA concentration in our healthy controls was approximately 6 µg/ml, and after 72 h of Cytosorb™ adsorber treatment, this level decreased to or to below 1 µg/ml. Consistent with these findings, SAA level in serum interfused with 31.25 µg/ml recombinant SAA was reduced to below 2 µg/ml after a 72 h treatment. Correspondingly, this strategy reduced HDL to less than one-tenth of the original level. According to this parallel elimination of SAA and HDL, it is supposed that most of the SAA was associated with HDL in the plasma and that they were removed by CytoSorb™ adsorber simultaneously. However, more investigations are needed to understand this process and further interpret the association between SAA and HDL during Cytosorb™ adsorber treatment.

The original concentrations of other substances including cholesterol, triglycerides, phospholipids, LDL and CRP, in this study were in the normal reference range. In addition, they were all reduced by Cytosorb™ adsorber treatment. The molecular weight of these substances varies from 25 kDa (CRP) to more than 300 kDa (HDL), and their removal cannot be explained by the size exclusion adsorb property of CytoSorb™ adsorber. A similar phenomenon was also found in a case report, in which cytokines with similar molecular weights had distinct removal rates by CytoSorb™ treatment[131]. Data for CytoSorb™ adsorber removing lipids and lipoproteins were not available in previous studies. Two case reports showed that

bilirubin was also greatly reduced by CytoSorb™ adsorber, which has a molecular weight of 584 kDa[128,131]. Many conditions in patients lead to changes in bilirubin levels, and we cannot exclude the possibility that Cytosorb™ adsorber can remove some high molecular weight materials.

Another issue that needs to be addressed is the much faster substances clean up speed in the final 24 h of CytoSorb™ adsorber treatment. During the treatment, samples from 5 treatment time points were collected, and bead columns were replaced by new ones after every 24 h. The sample volume was 10 ml at the very beginning, while at 48 h, only 4 ml plasma was left in the system. With the same CytoSorb™ adsorber volume, it is reasonable to have a faster elimination in the final 24 h. For the limited sample size, it is not possible to calculate the elimination rates of the substance in different treatment phases.

5 Conclusions

This study demonstrates that SAA is a proinflammatory mediator in macrophages. Compared to a traditional PAMP (LPS), SAA showed a strong induction of IL-1β, IL-6, MCP-1, NO production and ROS, which provides an explanation for the association found between the increased SAA and the growing cardiovascular complications in CKD patients.

TLR2 and TLR4 are two critical receptors for SAA-mediated cytokine and NO production. However, distinct patterns of those two receptors were observed in the production of different cytokines. For example, TLR2 and TLR4 play a more critical role in the early stage of SAA-induced MCP-1 production. Regardless of the stimulation time, SAA-generated IL-6 is more dependent on TLR4 and only partly on TLR2, whereas only TLR4 is responsible for SAA-induced IL-1β secretion. Moreover, antagonists of TLR2 and TLR4 show a substantial suppression of SAA-triggered NO production at both 24 h and 48 h stimulation. In summary, the SAA-triggered NO production is mainly dependent on TLR2 and TLR4, while in addition to these two receptors, other receptors might be simultaneously involved in SAA-mediated cytokine generation.

The NLRP3 inflammasome is included in this project for the intracellular signaling pathway investigation. This complex is only involved in the SAA-mediated IL-1β generation but not in SAA-induced IL-6, MCP-1 and NO production. These results are not consistent with previous studies, which have shown the essential role of IL-1β during MCP-1 and IL-6 production. The low level of IL-1β and limited stimulation time might be the reasons for this discrepancy. Other investigations, such as *in vivo* or *in vitro* experiments targeting the NLRP3 inflammasome, are required to further explore the role of IL-1β or the NLRP3 inflammasome in SAA-mediated IL-6 and MCP-1 production.

In this study, SAA could induce murine and human macrophages to generate intracellular ROS but could only promote murine macrophages produce mitochondrial ROS. ROS were found to play a critical role during NLRP3 inflammasome activation, especially the mitochondria derived ROS[133]. Whether

the low mitochondrial ROS level is responsible for the inefficiency of IL-1β release in THP-1 macrophages and the pathway for SAA triggering ROS need to be further explored.

These conclusions are also shown in the following Figure 20.

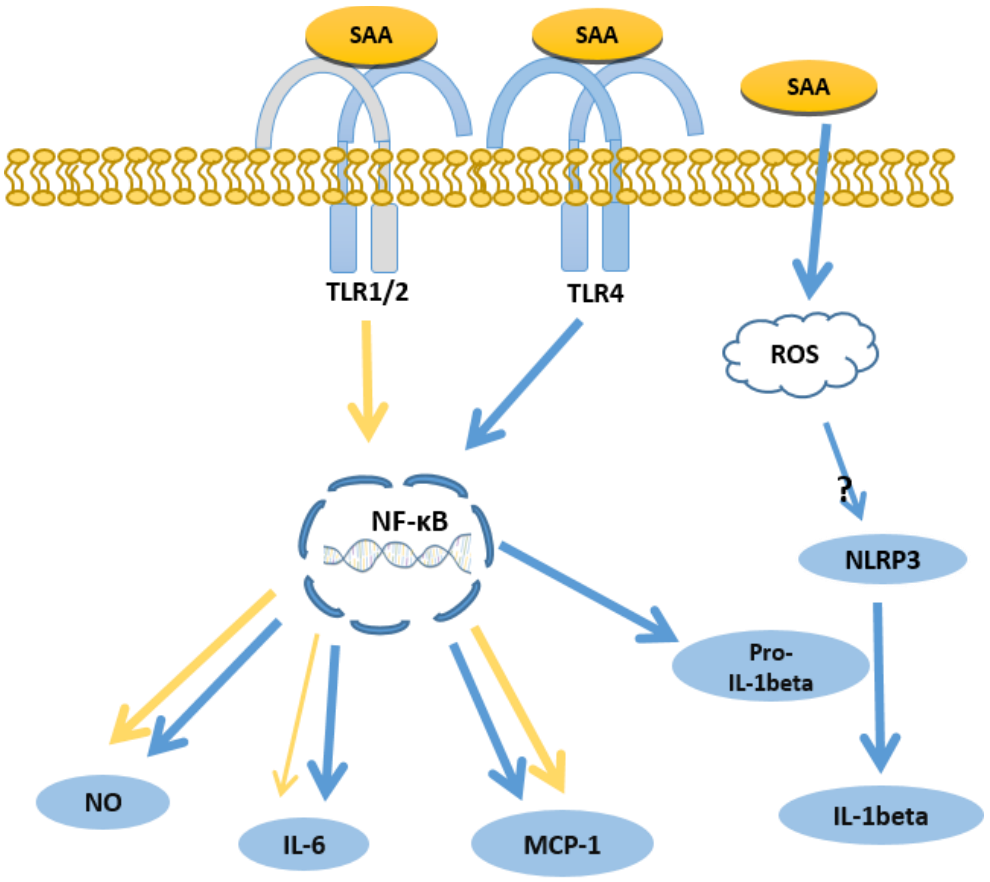

Figure 20 Signaling pathways for SAA-mediated inflammatory reactions in macrophages
IL, interleukin; MCP-1, monocyte chemoattractant protein 1; NF-κB, nuclear factor kappa-light-chain-enhancer of activated B cells; NLRP3, NOD-like receptor, pyrin domain containing 3; NO, nitric oxide; ROS, reactive oxygen species; SAA, serum amyloid A; TLR, Toll-like receptor.

Considering the significant proinflammatory properties of SAA, and the sustained elevated SAA in dialysis patients. It is necessary to explore methods to remove SAA from the circulation. A mini plasma adsorption system filled with CytoSorb^{TM} adsorber efficiently removed SAA from human plasma. However, CytoSorb^{TM} adsorber is not specific for SAA, and can adsorb other substances, such as protein, CRP, triglycerides and HDL-C. An investigation designed to evaluate the capacity

of CytoSorb™ adsorber or SAA removal in clinical treatment has been planned. We also look forward to the development of SAA-specific adsorbent material.

References

1 Mortality, G. B. D. & Causes of Death, C. Global, regional, and national life expectancy, all-cause mortality, and cause-specific mortality for 249 causes of death, 1980-2015: a systematic analysis for the Global Burden of Disease Study 2015. *Lancet* **388**, 1459-1544, doi:10.1016/S0140-6736(16)31012-1 (2016).

2 Zimmermann, J., Herrlinger, S., Pruy, A., Metzger, T. & Wanner, C. Inflammation enhances cardiovascular risk and mortality in hemodialysis patients. *Kidney international* **55**, 648-658, doi:10.1046/j.1523-1755.1999.00273.x (1999).

3 Stenvinkel, P., Heimburger, O., Paultre, F., Diczfalusy, U., Wang, T., Berglund, L. & Jogestrand, T. Strong association between malnutrition, inflammation, and atherosclerosis in chronic renal failure. *Kidney international* **55**, 1899-1911, doi:10.1046/j.1523-1755.1999.00422.x (1999).

4 Tolle, M., Huang, T., Schuchardt, M., Jankowski, V., Prufer, N., Jankowski, J., Tietge, U. J., Zidek, W. & van der Giet, M. High-density lipoprotein loses its anti-inflammatory capacity by accumulation of pro-inflammatory-serum amyloid A. *Cardiovascular research* **94**, 154-162, doi:10.1093/cvr/cvs089 (2012).

5 Han, C. Y., Tang, C., Guevara, M. E., Wei, H., Wietecha, T., Shao, B., Subramanian, S., Omer, M., Wang, S., O'Brien, K. D., Marcovina, S. M., Wight, T. N., Vaisar, T., de Beer, M. C., de Beer, F. C., Osborne, W. R., Elkon, K. B. & Chait, A. Serum amyloid A impairs the antiinflammatory properties of HDL. *J Clin Invest* **126**, 266-281, doi:10.1172/JCI83475 (2016).

6 Zewinger, S., Drechsler, C., Kleber, M. E., Dressel, A., Riffel, J., Triem, S., Lehmann, M., Kopecky, C., Saemann, M. D., Lepper, P. M., Silbernagel, G., Scharnagl, H., Ritsch, A., Thorand, B., de las Heras Gala, T., Wagenpfeil, S., Koenig, W., Peters, A., Laufs, U., Wanner, C., Fliser, D., Speer, T. & Marz, W. Serum amyloid A: high-density lipoproteins interaction and cardiovascular risk. *Eur Heart J* **36**, 3007-3016, doi:10.1093/eurheartj/ehv352 (2015).

7 Shainkin-Kestenbaum, R., Winikoff, Y. & Cristal, N. Serum amyloid A concentrations during the course of acute ischaemic heart disease. *J Clin Pathol* **39**, 635-637 (1986).

8 Whitehead, A. S., de Beer, M. C., Steel, D. M., Rits, M., Lelias, J. M., Lane, W. S. & de Beer, F. C. Identification of novel members of the serum amyloid A protein superfamily as constitutive apolipoproteins of high density lipoprotein. *J Biol Chem* **267**, 3862-3867 (1992).

9 Larson, M. A., Wei, S. H., Weber, A., Weber, A. T. & McDonald, T. L. *Induction of human mammary-associated serum amyloid A3 expression by prolactin or lipopolysaccharide* 301 thesis, (2003).

10 De Buck, M., Gouwy, M., Wang, J. M., Van Snick, J., Opdenakker, G., Struyf, S. & Van Damme, J. Structure and Expression of Different Serum Amyloid A (SAA) Variants and their Concentration-Dependent Functions During Host Insults. *Curr Med Chem* **23**, 1725-1755 (2016).

11 Betts, J. C., Cheshire, J. K., Akira, S., Kishimoto, T. & Woo, P. The role of NF-kappa B and NF-IL6 transactivating factors in the synergistic activation of human serum amyloid A gene expression by interleukin-1 and interleukin-6. *J Biol Chem* **268**, 25624-25631 (1993).

12 Raynes, J. G., Eagling, S. & McAdam, K. P. Acute-phase protein synthesis in human hepatoma cells: differential regulation of serum amyloid A (SAA) and haptoglobin by interleukin-1 and interleukin-6. *Clin Exp Immunol* **83**, 488-491 (1991).

13 Ishida, T., Matsuura, K., Setoguchi, M., Higuchi, Y. & Yamamoto, S. Enhancement of murine serum amyloid A3 mRNA expression by glucocorticoids and its regulation by cytokines. *J Leukoc Biol* **56**, 797-806 (1994).

14 Jiang, S. L., Lozanski, G., Samols, D. & Kushner, I. Induction of human serum amyloid A in Hep 3B cells by IL-6 and IL-1 beta involves both transcriptional and post-transcriptional mechanisms. *J Immunol* **154**, 825-831 (1995).

15 Jensen, L. E. & Whitehead, A. S. Regulation of serum amyloid A protein expression during the acute-phase response. *Biochem J* **334 (Pt 3)**, 489-503 (1998).

16 Abe, T., Kojima, M., Akanuma, S., Iwashita, H., Yamazaki, T., Okuyama, R., Ichikawa, K., Umemura, M., Nakano, H., Takahashi, S. & Takahashi, Y. N-terminal hydrophobic amino acids of activating transcription factor 5 (ATF5) protein confer interleukin 1beta (IL-1beta)-induced stabilization. *J Biol Chem* **289**, 3888-3900, doi:10.1074/jbc.M113.491217 (2014).

17 Cabana, V. G., Feng, N., Reardon, C. A., Lukens, J., Webb, N. R., de Beer, F. C. & Getz, G. S. Influence of apoA-I and apoE on the formation of serum amyloid A-containing lipoproteins in vivo and in vitro. *J Lipid Res* **45**, 317-325, doi:10.1194/jlr.M300414-JLR200 (2004).

18 Sato, M., Ohkawa, R., Yoshimoto, A., Yano, K., Ichimura, N., Nishimori, M., Okubo, S., Yatomi, Y. & Tozuka, M. Effects of serum amyloid A on the structure and antioxidant ability of high-density lipoprotein. *Biosci Rep* **36**, doi:10.1042/BSR20160075 (2016).

19 Jayaraman, S., Haupt, C. & Gursky, O. Thermal transitions in serum amyloid A in solution and on the lipid: implications for structure and stability of acute-phase HDL. *J Lipid Res* **56**, 1531-1542, doi:10.1194/jlr.M059162 (2015).

20 Frame, N. M. & Gursky, O. Structure of serum amyloid A suggests a mechanism for selective lipoprotein binding and functions: SAA as a hub in macromolecular interaction networks. *FEBS Lett* **590**, 866-879, doi:10.1002/1873-3468.12116 (2016).

21 Hoffman, J. S. & Benditt, E. P. Plasma clearance kinetics of the amyloid-related high density lipoprotein apoprotein, serum amyloid protein (apoSAA), in the mouse. Evidence for rapid apoSAA clearance. *J Clin Invest* **71**, 926-934 (1983).

22 Meek, R. L., Eriksen, N. & Benditt, E. P. Serum amyloid A in the mouse. Sites of uptake and mRNA expression. *Am J Pathol* **135**, 411-419 (1989).

23 Niemi, K., Baumann, M. H., Kovanen, P. T. & Eklund, K. K. Serum amyloid A (SAA) activates human mast cells which leads into degradation of SAA and generation of an amyloidogenic SAA fragment. *Biochim Biophys Acta* **1762**, 424-430, doi:10.1016/j.bbadis.2006.01.001 (2006).

24 Migita, K., Yamasaki, S., Shibatomi, K., Ida, H., Kita, M., Kawakami, A. & Eguchi, K. Impaired degradation of serum amyloid A (SAA) protein by cytokine-stimulated monocytes. *Clin Exp Immunol* **123**, 408-411 (2001).

25 Gollaher, C. J. & Bausserman, L. L. Hepatic catabolism of serum amyloid A during an acute phase response and chronic inflammation. *Proc Soc Exp Biol Med* **194**, 245-250 (1990).

26 van der Hilst, J. C., Yamada, T., Op den Camp, H. J., van der Meer, J. W., Drenth, J. P. & Simon, A. Increased susceptibility of serum amyloid A 1.1 to degradation by MMP-1: potential explanation for higher risk of type AA amyloidosis. *Rheumatology (Oxford)* **47**, 1651-1654, doi:10.1093/rheumatology/ken371 (2008).

27 Linke, R. P., Meinel, A., Chalcroft, J. P. & Urieli-Shoval, S. Serum amyloid A (SAA) treatment enhances the recovery of aggravated polymicrobial sepsis in mice, whereas blocking SAA's invariant peptide results in early death. *Amyloid* **24**, 149-150, doi:10.1080/13506129.2017.1295950 (2017).

28 Hari-Dass, R., Shah, C., Meyer, D. J. & Raynes, J. G. Serum amyloid A protein binds to outer membrane protein A of gram-negative bacteria. *J Biol Chem* **280**, 18562-18567, doi:10.1074/jbc.M500490200 (2005).

29 Murdoch, C. C., Espenschied, S. T., Matty, M. A., Mueller, O., Tobin, D. M. & Rawls, J. F. Intestinal Serum amyloid A suppresses systemic neutrophil activation and bactericidal activity in response to microbiota colonization. *PLoS Pathog* **15**, e1007381, doi:10.1371/journal.ppat.1007381 (2019).

30 Cai, Z., Cai, L., Jiang, J., Chang, K. S., van der Westhuyzen, D. R. & Luo, G. Human serum amyloid A protein inhibits hepatitis C virus entry into cells. *J Virol* **81**, 6128-6133, doi:10.1128/JVI.02627-06 (2007).

31 Lavie, M., Voisset, C., Vu-Dac, N., Zurawski, V., Duverlie, G., Wychowski, C. & Dubuisson, J. Serum amyloid A has antiviral activity against hepatitis C virus by inhibiting virus entry in a cell culture system. *Hepatology* **44**, 1626-1634, doi:10.1002/hep.21406 (2006).

32 Derebe, M. G., Zlatkov, C. M., Gattu, S., Ruhn, K. A., Vaishnava, S., Diehl, G. E., MacMillan, J. B., Williams, N. S. & Hooper, L. V. Serum amyloid A is a retinol binding protein that transports retinol during bacterial infection. *Elife* **3**, e03206, doi:10.7554/eLife.03206 (2014).

33 Sun, L., Zhou, H., Zhu, Z., Yan, Q., Wang, L., Liang, Q. & Ye, R. D. Ex vivo and in vitro effect of serum amyloid a in the induction of macrophage M2 markers and efferocytosis of apoptotic neutrophils. *J Immunol* **194**, 4891-4900, doi:10.4049/jimmunol.1402164 (2015).

34 Aldo-Benson, M. A. & Benson, M. D. SAA suppression of immune response in vitro: evidence for an effect on T cell-macrophage interaction. *J Immunol* **128**, 2390-2392 (1982).

35 Connolly, M., Rooney, P. R., McGarry, T., Maratha, A. X., McCormick, J., Miggin, S. M., Veale, D. J. & Fearon, U. Acute serum amyloid A is an endogenous TLR2 ligand that mediates inflammatory and angiogenic mechanisms. *Ann Rheum Dis* **75**, 1392-1398, doi:10.1136/annrheumdis-2015-207655 (2016).

36 Lakota, K., Mrak-Poljsak, K., Bozic, B., Tomsic, M. & Sodin-Semrl, S. Serum amyloid A activation of human coronary artery endothelial cells exhibits a neutrophil promoting molecular profile. *Microvasc Res* **90**, 55-63, doi:10.1016/j.mvr.2013.07.011 (2013).

37 Connelly, M. A. & Williams, D. L. Scavenger receptor BI: a scavenger receptor with a mission to transport high density lipoprotein lipids. *Curr Opin Lipidol* **15**, 287-295 (2004).

38 Baillie, A. G., Coburn, C. T. & Abumrad, N. A. Reversible binding of long-chain fatty acids to purified FAT, the adipose CD36 homolog. *J Membr Biol* **153**, 75-81 (1996).

39 Fukami, K., Taguchi, K., Yamagishi, S. & Okuda, S. Receptor for advanced glycation endproducts and progressive kidney disease. *Curr Opin Nephrol Hypertens* **24**, 54-60, doi:10.1097/MNH.0000000000000091 (2015).

40 He, H. Q. & Ye, R. D. The Formyl Peptide Receptors: Diversity of Ligands and Mechanism for Recognition. *Molecules* **22**, doi:10.3390/molecules22030455 (2017).

41 Adinolfi, E., Giuliani, A. L., De Marchi, E., Pegoraro, A., Orioli, E. & Di Virgilio, F. The P2X7 receptor: A main player in inflammation. *Biochem Pharmacol* **151**, 234-244, doi:10.1016/j.bcp.2017.12.021 (2018).

42 He, R. L., Zhou, J., Hanson, C. Z., Chen, J., Cheng, N. & Ye, R. D. Serum amyloid A induces G-CSF expression and neutrophilia via Toll-like receptor 2. *Blood* **113**, 429-437, doi:10.1182/blood-2008-03-139923 (2009).

43 Sun, L., Zhu, Z., Cheng, N., Yan, Q. & Ye, R. D. Serum amyloid A induces interleukin-33 expression through an IRF7-dependent pathway. *Eur J Immunol* **44**, 2153-2164, doi:10.1002/eji.201344310 (2014).

44 Passey, S. L., Bozinovski, S., Vlahos, R., Anderson, G. P. & Hansen, M. J. Serum Amyloid A Induces Toll-Like Receptor 2-Dependent Inflammatory Cytokine Expression and Atrophy in C2C12 Skeletal Muscle Myotubes. *PloS one* **11**, e0146882, doi:10.1371/journal.pone.0146882 (2016).

45 O'Reilly, S., Cant, R., Ciechomska, M., Finnigan, J., Oakley, F., Hambleton, S. & van Laar, J. M. Serum amyloid A induces interleukin-6 in dermal fibroblasts via Toll-like receptor 2, interleukin-1 receptor-associated kinase 4 and nuclear factor-kappaB. *Immunology* **143**, 331-340, doi:10.1111/imm.12260 (2014).

46 Zhou, H., Chen, M., Zhang, G. & Ye, R. D. Suppression of Lipopolysaccharide-Induced Inflammatory Response by Fragments from Serum Amyloid A. *J Immunol* **199**, 1105-1112, doi:10.4049/jimmunol.1700470 (2017).

47 Choi, M., Kim, M. O., Lee, J., Jeong, J., Sung, Y., Park, S., Kwon, W., Jang, S., Park, S. J., Kim, H. S., Jang, W. Y., Kim, S. H., Lee, S., Choi, S. K. & Ryoo, Z. Y. Hepatic serum amyloid A1

upregulates interleukin-17 (IL-17) in gammadelta T cells through Toll-like receptor 2 and is associated with psoriatic symptoms in transgenic mice. *Scand J Immunol* **89**, e12764, doi:10.1111/sji.12764 (2019).

48 Yu, N., Liu, S., Yi, X., Zhang, S. & Ding, Y. Serum amyloid A induces interleukin-1beta secretion from keratinocytes via the NACHT, LRR and PYD domains-containing protein 3 inflammasome. *Clin Exp Immunol* **179**, 344-353, doi:10.1111/cei.12458 (2015).

49 Niemi, K., Teirila, L., Lappalainen, J., Rajamaki, K., Baumann, M. H., Oorni, K., Wolff, H., Kovanen, P. T., Matikainen, S. & Eklund, K. K. Serum amyloid A activates the NLRP3 inflammasome via P2X7 receptor and a cathepsin B-sensitive pathway. *J Immunol* **186**, 6119-6128, doi:10.4049/jimmunol.1002843 (2011).

50 Li, W., Zhu, S., Li, J., D'Amore, J., D'Angelo, J., Yang, H., Wang, P., Tracey, K. J. & Wang, H. Serum Amyloid A Stimulates PKR Expression and HMGB1 Release Possibly through TLR4/RAGE Receptors. *Mol Med* **21**, 515-525, doi:10.2119/molmed.2015.00109 (2015).

51 de Seny, D., Cobraiville, G., Charlier, E., Neuville, S., Esser, N., Malaise, D., Malaise, O., Calvo, F. Q., Relic, B. & Malaise, M. G. Acute-phase serum amyloid a in osteoarthritis: regulatory mechanism and proinflammatory properties. *PloS one* **8**, e66769, doi:10.1371/journal.pone.0066769 (2013).

52 Deguchi, A., Tomita, T., Omori, T., Komatsu, A., Ohto, U., Takahashi, S., Tanimura, N., Akashi-Takamura, S., Miyake, K. & Maru, Y. Serum amyloid A3 binds MD-2 to activate p38 and NF-kappaB pathways in a MyD88-dependent manner. *J Immunol* **191**, 1856-1864, doi:10.4049/jimmunol.1201996 (2013).

53 He, R., Sang, H. & Ye, R. D. Serum amyloid A induces IL-8 secretion through a G protein-coupled receptor, FPRL1/LXA4R. *Blood* **101**, 1572-1581, doi:10.1182/blood-2002-05-1431 (2003).

54 Anthony, D., Seow, H. J., Uddin, M., Thompson, M., Dousha, L., Vlahos, R., Irving, L. B., Levy, B. D., Anderson, G. P. & Bozinovski, S. Serum amyloid A promotes lung neutrophilia by increasing IL-17A levels in the mucosa and gammadelta T cells. *Am J Respir Crit Care Med* **188**, 179-186, doi:10.1164/rccm.201211-2139OC (2013).

55 Bozinovski, S., Uddin, M., Vlahos, R., Thompson, M., McQualter, J. L., Merritt, A. S., Wark, P. A., Hutchinson, A., Irving, L. B., Levy, B. D. & Anderson, G. P. Serum amyloid A opposes lipoxin A(4) to mediate glucocorticoid refractory lung inflammation in chronic obstructive pulmonary disease. *Proc Natl Acad Sci U S A* **109**, 935-940, doi:10.1073/pnas.1109382109 (2012).

56 Mullan, R. H., McCormick, J., Connolly, M., Bresnihan, B., Veale, D. J. & Fearon, U. A role for the high-density lipoprotein receptor SR-B1 in synovial inflammation via serum amyloid-A. *Am J Pathol* **176**, 1999-2008, doi:10.2353/ajpath.2010.090014 (2010).

57 Connolly, M., Mullan, R. H., McCormick, J., Matthews, C., Sullivan, O., Kennedy, A., FitzGerald, O., Poole, A. R., Bresnihan, B., Veale, D. J. & Fearon, U. Acute-phase serum amyloid A regulates tumor necrosis factor alpha and matrix turnover and predicts disease progression in patients with

inflammatory arthritis before and after biologic therapy. *Arthritis Rheum* **64**, 1035-1045, doi:10.1002/art.33455 (2012).

58 Okamoto, H., Katagiri, Y., Kiire, A., Momohara, S. & Kamatani, N. Serum amyloid A activates nuclear factor-kappaB in rheumatoid synovial fibroblasts through binding to receptor of advanced glycation end-products. *J Rheumatol* **35**, 752-756 (2008).

59 Baranova, I. N., Bocharov, A. V., Vishnyakova, T. G., Kurlander, R., Chen, Z., Fu, D., Arias, I. M., Csako, G., Patterson, A. P. & Eggerman, T. L. CD36 is a novel serum amyloid A (SAA) receptor mediating SAA binding and SAA-induced signaling in human and rodent cells. *J Biol Chem* **285**, 8492-8506, doi:10.1074/jbc.M109.007526 (2010).

60 Schindler, R., Ghezzi, P. & Dinarello, C. A. IL-1 induces IL-1. IV. IFN-gamma suppresses IL-1 but not lipopolysaccharide-induced transcription of IL-1. *J Immunol* **144**, 2216-2222 (1990).

61 Zheng, H., Fletcher, D., Kozak, W., Jiang, M., Hofmann, K. J., Conn, C. A., Soszynski, D., Grabiec, C., Trumbauer, M. E., Shaw, A. & et al. Resistance to fever induction and impaired acute-phase response in interleukin-1 beta-deficient mice. *Immunity* **3**, 9-19 (1995).

62 Dinarello, C. A., Ikejima, T., Warner, S. J., Orencole, S. F., Lonnemann, G., Cannon, J. G. & Libby, P. Interleukin 1 induces interleukin 1. I. Induction of circulating interleukin 1 in rabbits in vivo and in human mononuclear cells in vitro. *J Immunol* **139**, 1902-1910 (1987).

63 Dinarello, C. A. Overview of the IL-1 family in innate inflammation and acquired immunity. *Immunol Rev* **281**, 8-27, doi:10.1111/imr.12621 (2018).

64 Hogquist, K. A., Unanue, E. R. & Chaplin, D. D. Release of IL-1 from mononuclear phagocytes. *J Immunol* **147**, 2181-2186 (1991).

65 Elliott, E. I. & Sutterwala, F. S. Initiation and perpetuation of NLRP3 inflammasome activation and assembly. *Immunol Rev* **265**, 35-52, doi:10.1111/imr.12286 (2015).

66 Perregaux, D. & Gabel, C. A. Interleukin-1 beta maturation and release in response to ATP and nigericin. Evidence that potassium depletion mediated by these agents is a necessary and common feature of their activity. *J Biol Chem* **269**, 15195-15203 (1994).

67 Pires, S. & Parker, D. IL-1beta activation in response to Staphylococcus aureus lung infection requires inflammasome-dependent and independent mechanisms. *Eur J Immunol* **48**, 1707-1716, doi:10.1002/eji.201847556 (2018).

68 Shridas, P., De Beer, M. C. & Webb, N. R. High-density lipoprotein inhibits serum amyloid A-mediated reactive oxygen species generation and NLRP3 inflammasome activation. *J Biol Chem* **293**, 13257-13269, doi:10.1074/jbc.RA118.002428 (2018).

69 Jabaut, J., Ather, J. L., Taracanova, A., Poynter, M. E. & Ckless, K. Mitochondria-targeted drugs enhance Nlrp3 inflammasome-dependent IL-1beta secretion in association with alterations in cellular redox and energy status. *Free Radic Biol Med* **60**, 233-245, doi:10.1016/j.freeradbiomed.2013.01.025 (2013).

70 Gabay, C. & Kushner, I. Acute-phase proteins and other systemic responses to inflammation. *N Engl J Med* **340**, 448-454, doi:10.1056/NEJM199902113400607 (1999).

71 Tanaka, T., Narazaki, M. & Kishimoto, T. IL-6 in inflammation, immunity, and disease. *Cold Spring Harb Perspect Biol* **6**, a016295, doi:10.1101/cshperspect.a016295 (2014).

72 Yadav, A., Saini, V. & Arora, S. MCP-1: chemoattractant with a role beyond immunity: a review. *Clin Chim Acta* **411**, 1570-1579, doi:10.1016/j.cca.2010.07.006 (2010).

73 Song, C., Hsu, K., Yamen, E., Yan, W., Fock, J., Witting, P. K., Geczy, C. L. & Freedman, S. B. Serum amyloid A induction of cytokines in monocytes/macrophages and lymphocytes. *Atherosclerosis* **207**, 374-383, doi:10.1016/j.atherosclerosis.2009.05.007 (2009).

74 Hirano, S., Zhou, Q., Furuyama, A. & Kanno, S. Differential Regulation of IL-1beta and IL-6 Release in Murine Macrophages. *Inflammation* **40**, 1933-1943, doi:10.1007/s10753-017-0634-1 (2017).

75 Reshetnikov, V., Hahn, J., Maueroder, C., Czegley, C., Munoz, L. E., Herrmann, M., Hoffmann, M. H. & Mokhir, A. Chemical Tools for Targeted Amplification of Reactive Oxygen Species in Neutrophils. *Front Immunol* **9**, 1827, doi:10.3389/fimmu.2018.01827 (2018).

76 Kattoor, A. J., Pothineni, N. V. K., Palagiri, D. & Mehta, J. L. Oxidative Stress in Atherosclerosis. *Curr Atheroscler Rep* **19**, 42, doi:10.1007/s11883-017-0678-6 (2017).

77 Santos, C. X., Tanaka, L. Y., Wosniak, J. & Laurindo, F. R. Mechanisms and implications of reactive oxygen species generation during the unfolded protein response: roles of endoplasmic reticulum oxidoreductases, mitochondrial electron transport, and NADPH oxidase. *Antioxid Redox Signal* **11**, 2409-2427, doi:10.1089/ARS.2009.2625 (2009).

78 Zhang, J., Wang, X., Vikash, V., Ye, Q., Wu, D., Liu, Y. & Dong, W. ROS and ROS-Mediated Cellular Signaling. *Oxid Med Cell Longev* **2016**, 4350965, doi:10.1155/2016/4350965 (2016).

79 Sho, T. & Xu, J. Role and mechanism of ROS scavengers in alleviating NLRP3-mediated inflammation. *Biotechnol Appl Biochem*, doi:10.1002/bab.1700 (2018).

80 Hatanaka, E., Dermargos, A., Armelin, H. A., Curi, R. & Campa, A. Serum amyloid A induces reactive oxygen species (ROS) production and proliferation of fibroblast. *Clin Exp Immunol* **163**, 362-367, doi:10.1111/j.1365-2249.2010.04300.x (2011).

81 Lei, J., Vodovotz, Y., Tzeng, E. & Billiar, T. R. Nitric oxide, a protective molecule in the cardiovascular system. *Nitric Oxide* **35**, 175-185, doi:10.1016/j.niox.2013.09.004 (2013).

82 Lee, M., Rey, K., Besler, K., Wang, C. & Choy, J. Immunobiology of Nitric Oxide and Regulation of Inducible Nitric Oxide Synthase. *Results Probl Cell Differ* **62**, 181-207, doi:10.1007/978-3-319-54090-0_8 (2017).

83 Perrotta, C., Cervia, D., Di Renzo, I., Moscheni, C., Bassi, M. T., Campana, L., Martelli, C., Catalani, E., Giovarelli, M., Zecchini, S., Coazzoli, M., Capobianco, A., Ottobrini, L., Lucignani, G., Rosa, P., Rovere-Querini, P., De Palma, C. & Clementi, E. Nitric Oxide Generated by Tumor-Associated

Macrophages Is Responsible for Cancer Resistance to Cisplatin and Correlated With Syntaxin 4 and Acid Sphingomyelinase Inhibition. *Front Immunol* **9**, 1186, doi:10.3389/fimmu.2018.01186 (2018).

84 Venkataramana, S., Lourenssen, S., Miller, K. G. & Blennerhassett, M. G. Early inflammatory damage to intestinal neurons occurs via inducible nitric oxide synthase. *Neurobiol Dis* **75**, 40-52, doi:10.1016/j.nbd.2014.12.014 (2015).

85 Fite, A., Abou-Samra, A. B. & Seyoum, B. Macrophages inhibit insulin signalling in adipocytes: role of inducible nitric oxide synthase and nitric oxide. *Can J Diabetes* **39**, 36-43, doi:10.1016/j.jcjd.2014.02.023 (2015).

86 Ren, D., Sun, R. & Wang, S. Role of inducible nitric oxide synthase expressed by alveolar macrophages in high mobility group box 1--induced acute lung injury. *Inflamm Res* **55**, 207-215, doi:10.1007/s00011-006-0072-2 (2006).

87 Huang, H., Koelle, P., Fendler, M., Schrottle, A., Czihal, M., Hoffmann, U., Conrad, M. & Kuhlencordt, P. J. Induction of inducible nitric oxide synthase (iNOS) expression by oxLDL inhibits macrophage derived foam cell migration. *Atherosclerosis* **235**, 213-222, doi:10.1016/j.atherosclerosis.2014.04.020 (2014).

88 Sigala, F., Savvari, P., Liontos, M., Sigalas, P., Pateras, I. S., Papalampros, A., Basdra, E. K., Kolettas, E., Papavassiliou, A. G. & Gorgoulis, V. G. Increased expression of bFGF is associated with carotid atherosclerotic plaques instability engaging the NF-kappaB pathway. *J Cell Mol Med* **14**, 2273-2280, doi:10.1111/j.1582-4934.2010.01082.x (2010).

89 Witting, P. K., Song, C., Hsu, K., Hua, S., Parry, S. N., Aran, R., Geczy, C. & Freedman, S. B. The acute-phase protein serum amyloid A induces endothelial dysfunction that is inhibited by high-density lipoprotein. *Free Radic Biol Med* **51**, 1390-1398, doi:10.1016/j.freeradbiomed.2011.06.031 (2011).

90 Zhu, S., Wang, Y., Chen, W., Li, W., Wang, A., Wong, S., Bao, G., Li, J., Yang, H., Tracey, K. J., D'Angelo, J. & Wang, H. High-Density Lipoprotein (HDL) Counter-Regulates Serum Amyloid A (SAA)-Induced sPLA2-IIE and sPLA2-V Expression in Macrophages. *PloS one* **11**, e0167468, doi:10.1371/journal.pone.0167468 (2016).

91 Jovanovic, D. B., Stosovic, M. D., Gojakovic, B. M., Jovanovic, N. Z., Stanojevic-Stosovic, M., Simic-Ogrizovic, S. P. & Naumovic, R. T. Inflammatory markers as mortality predictors in continuous ambulatory peritoneal dialysis patients. *Ren Fail* **37**, 230-236, doi:10.3109/0886022X.2014.982478 (2015).

92 Duranton, F., Cohen, G., De Smet, R., Rodriguez, M., Jankowski, J., Vanholder, R., Argiles, A. & European Uremic Toxin Work, G. Normal and pathologic concentrations of uremic toxins. *J Am Soc Nephrol* **23**, 1258-1270, doi:10.1681/ASN.2011121175 (2012).

93 Bonomini, M., Sirolli, V., Pieroni, L., Felaco, P., Amoroso, L. & Urbani, A. Proteomic Investigations into Hemodialysis Therapy. *Int J Mol Sci* **16**, 29508-29521, doi:10.3390/ijms161226189 (2015).

94 Chen, G. M., Lan, Y. Y., Wang, C. F., Zhan, H. X., Wang, W. R., Chen, J. H. & Chen, J. Clearance of serum solutes by hemofiltration in dogs with severe heat stroke. *Scand J Trauma Resusc Emerg Med* **22**, 49, doi:10.1186/s13049-014-0049-z (2014).

95 Borthwick, E. M., Hill, C. J., Rabindranath, K. S., Maxwell, A. P., McAuley, D. F. & Blackwood, B. High-volume haemofiltration for sepsis. *Cochrane Database Syst Rev*, CD008075, doi:10.1002/14651858.CD008075.pub2 (2013).

96 Kade, G., Lubas, A., Rzeszotarska, A., Korsak, J. & Niemczyk, S. Effectiveness of High Cut-Off Hemofilters in the Removal of Selected Cytokines in Patients During Septic Shock Accompanied by Acute Kidney Injury-Preliminary Study. *Med Sci Monit* **22**, 4338-4344, doi:10.12659/MSM.896819 (2016).

97 Gruda, M. C., Ruggeberg, K. G., O'Sullivan, P., Guliashvili, T., Scheirer, A. R., Golobish, T. D., Capponi, V. J. & Chan, P. P. Broad adsorption of sepsis-related PAMP and DAMP molecules, mycotoxins, and cytokines from whole blood using CytoSorb(R) sorbent porous polymer beads. *PloS one* **13**, e0191676, doi:10.1371/journal.pone.0191676 (2018).

98 David, S., Thamm, K., Schmidt, B. M., Falk, C. S. & Kielstein, J. T. Effect of extracorporeal cytokine removal on vascular barrier function in a septic shock patient. *J Intensive Care* **5**, 12, doi:10.1186/s40560-017-0208-1 (2017).

99 Moore, K. J., Sheedy, F. J. & Fisher, E. A. Macrophages in atherosclerosis: a dynamic balance. *Nat Rev Immunol* **13**, 709-721, doi:10.1038/nri3520 (2013).

100 Mangan, M. S. J., Olhava, E. J., Roush, W. R., Seidel, H. M., Glick, G. D. & Latz, E. Targeting the NLRP3 inflammasome in inflammatory diseases. *Nat Rev Drug Discov* **17**, 588-606, doi:10.1038/nrd.2018.97 (2018).

101 Kuwata, H., Yuzurihara, C., Kinoshita, N., Taki, Y., Ikegami, Y., Washio, S., Hirakawa, Y., Yoda, E., Aiuchi, T., Itabe, H., Nakatani, Y. & Hara, S. The group VIA calcium-independent phospholipase A2 and NFATc4 pathway mediates IL-1beta-induced expression of chemokines CCL2 and CXCL10 in rat fibroblasts. *FEBS J* **285**, 2056-2070, doi:10.1111/febs.14462 (2018).

102 Vanhoutte, P. M., Shimokawa, H., Feletou, M. & Tang, E. H. Endothelial dysfunction and vascular disease - a 30th anniversary update. *Acta Physiol (Oxf)* **219**, 22-96, doi:10.1111/apha.12646 (2017).

103 Brunner, M., Gruber, M., Schmid, D., Baran, H. & Moeslinger, T. Proliferation of macrophages due to the inhibition of inducible nitric oxide synthesis by oxidized low-density lipoproteins. *EXCLI J* **14**, 439-451, doi:10.17179/excli2015-151 (2015).

104 Abdul-Cader, M. S., Amarasinghe, A. & Abdul-Careem, M. F. Activation of toll-like receptor signaling pathways leading to nitric oxide-mediated antiviral responses. *Arch Virol* **161**, 2075-2086, doi:10.1007/s00705-016-2904-x (2016).

105 Sandri, S., Rodriguez, D., Gomes, E., Monteiro, H. P., Russo, M. & Campa, A. Is serum amyloid A an endogenous TLR4 agonist? *J Leukoc Biol* **83**, 1174-1180, doi:10.1189/jlb.0407203 (2008).

106 Kleinert, H., Wallerath, T., Fritz, G., Ihrig-Biedert, I., Rodriguez-Pascual, F., Geller, D. A. & Forstermann, U. Cytokine induction of NO synthase II in human DLD-1 cells: roles of the JAK-STAT, AP-1 and NF-kappaB-signaling pathways. *British journal of pharmacology* **125**, 193-201, doi:10.1038/sj.bjp.0702039 (1998).

107 Benson, M. D. & Cohen, A. S. Serum amyloid A protein in amyloidosis, rheumatic, and enoplastic diseases. *Arthritis Rheum* **22**, 36-42 (1979).

108 Benditt, E. P., Eriksen, N. & Hanson, R. H. Amyloid protein SAA is an apoprotein of mouse plasma high density lipoprotein. *Proc Natl Acad Sci U S A* **76**, 4092-4096, doi:10.1073/pnas.76.8.4092 (1979).

109 Bjorkman, L., Raynes, J. G., Shah, C., Karlsson, A., Dahlgren, C. & Bylund, J. The proinflammatory activity of recombinant serum amyloid A is not shared by the endogenous protein in the circulation. *Arthritis Rheum* **62**, 1660-1665, doi:10.1002/art.27440 (2010).

110 Opal, S. M., Scannon, P. J., Vincent, J. L., White, M., Carroll, S. F., Palardy, J. E., Parejo, N. A., Pribble, J. P. & Lemke, J. H. Relationship between plasma levels of lipopolysaccharide (LPS) and LPS-binding protein in patients with severe sepsis and septic shock. *J Infect Dis* **180**, 1584-1589, doi:10.1086/315093 (1999).

111 Ghonime, M. G., Shamaa, O. R., Das, S., Eldomany, R. A., Fernandes-Alnemri, T., Alnemri, E. S., Gavrilin, M. A. & Wewers, M. D. Inflammasome priming by lipopolysaccharide is dependent upon ERK signaling and proteasome function. *J Immunol* **192**, 3881-3888, doi:10.4049/jimmunol.1301974 (2014).

112 Cheng, N., He, R., Tian, J., Ye, P. P. & Ye, R. D. Cutting edge: TLR2 is a functional receptor for acute-phase serum amyloid A. *J Immunol* **181**, 22-26 (2008).

113 Ather, J. L., Ckless, K., Martin, R., Foley, K. L., Suratt, B. T., Boyson, J. E., Fitzgerald, K. A., Flavell, R. A., Eisenbarth, S. C. & Poynter, M. E. Serum amyloid A activates the NLRP3 inflammasome and promotes Th17 allergic asthma in mice. *J Immunol* **187**, 64-73, doi:10.4049/jimmunol.1100500 (2011).

114 Coll, R. C., Robertson, A. A., Chae, J. J., Higgins, S. C., Munoz-Planillo, R., Inserra, M. C., Vetter, I., Dungan, L. S., Monks, B. G., Stutz, A., Croker, D. E., Butler, M. S., Haneklaus, M., Sutton, C. E., Nunez, G., Latz, E., Kastner, D. L., Mills, K. H., Masters, S. L., Schroder, K., Cooper, M. A. & O'Neill, L. A. A small-molecule inhibitor of the NLRP3 inflammasome for the treatment of inflammatory diseases. *Nat Med* **21**, 248-255, doi:10.1038/nm.3806 (2015).

115 Perera, A. P., Fernando, R., Shinde, T., Gundamaraju, R., Southam, B., Sohal, S. S., Robertson, A. A. B., Schroder, K., Kunde, D. & Eri, R. MCC950, a specific small molecule inhibitor of NLRP3 inflammasome attenuates colonic inflammation in spontaneous colitis mice. *Sci Rep* **8**, 8618, doi:10.1038/s41598-018-26775-w (2018).

116 Coeshott, C., Ohnemus, C., Pilyavskaya, A., Ross, S., Wieczorek, M., Kroona, H., Leimer, A. H. & Cheronis, J. Converting enzyme-independent release of tumor necrosis factor alpha and IL-1beta

from a stimulated human monocytic cell line in the presence of activated neutrophils or purified proteinase 3. *Proc Natl Acad Sci U S A* **96**, 6261-6266, doi:10.1073/pnas.96.11.6261 (1999).

117 Hunter, C. A. & Jones, S. A. IL-6 as a keystone cytokine in health and disease. *Nat Immunol* **16**, 448-457, doi:10.1038/ni.3153 (2015).

118 Murayama, R., Kobayashi, M., Takeshita, A., Yasui, T. & Yamamoto, M. MAPKs, activator protein-1 and nuclear factor-kappaB mediate production of interleukin-1beta-stimulated cytokines, prostaglandin E(2) and MMP-1 in human periodontal ligament cells. *J Periodontal Res* **46**, 568-575, doi:10.1111/j.1600-0765.2011.01374.x (2011).

119 Shindo, S., Hosokawa, Y., Hosokawa, I., Ozaki, K. & Matsuo, T. Genipin inhibits IL-1beta-induced CCL20 and IL-6 production from human periodontal ligament cells. *Cell Physiol Biochem* **33**, 357-364, doi:10.1159/000356675 (2014).

120 Schuchardt, M., Prufer, N., Tu, Y., Herrmann, J., Hu, X. P., Chebli, S., Dahlke, K., Zidek, W., van der Giet, M. & Tolle, M. Dysfunctional high-density lipoprotein activates toll-like receptors via serum amyloid A in vascular smooth muscle cells. *Sci Rep* **9**, 3421, doi:10.1038/s41598-019-39846-3 (2019).

121 Wong, H. S., Jaumouille, V., Freeman, S. A., Doodnauth, S. A., Schlam, D., Canton, J., Mukovozov, I. M., Saric, A., Grinstein, S. & Robinson, L. A. Chemokine Signaling Enhances CD36 Responsiveness toward Oxidized Low-Density Lipoproteins and Accelerates Foam Cell Formation. *Cell Rep* **14**, 2859-2871, doi:10.1016/j.celrep.2016.02.071 (2016).

122 Wiesner, P., Tafelmeier, M., Chittka, D., Choi, S. H., Zhang, L., Byun, Y. S., Almazan, F., Yang, X., Iqbal, N., Chowdhury, P., Maisel, A., Witztum, J. L., Handel, T. M., Tsimikas, S. & Miller, Y. I. MCP-1 binds to oxidized LDL and is carried by lipoprotein(a) in human plasma. *J Lipid Res* **54**, 1877-1883, doi:10.1194/jlr.M036343 (2013).

123 Roshan, M. H., Tambo, A. & Pace, N. P. The Role of TLR2, TLR4, and TLR9 in the Pathogenesis of Atherosclerosis. *Int J Inflam* **2016**, 1532832, doi:10.1155/2016/1532832 (2016).

124 Mridha, A. R., Wree, A., Robertson, A. A. B., Yeh, M. M., Johnson, C. D., Van Rooyen, D. M., Haczeyni, F., Teoh, N. C., Savard, C., Ioannou, G. N., Masters, S. L., Schroder, K., Cooper, M. A., Feldstein, A. E. & Farrell, G. C. NLRP3 inflammasome blockade reduces liver inflammation and fibrosis in experimental NASH in mice. *J Hepatol* **66**, 1037-1046, doi:10.1016/j.jhep.2017.01.022 (2017).

125 Chan, G. C., Fish, J. E., Mawji, I. A., Leung, D. D., Rachlis, A. C. & Marsden, P. A. Epigenetic basis for the transcriptional hyporesponsiveness of the human inducible nitric oxide synthase gene in vascular endothelial cells. *J Immunol* **175**, 3846-3861 (2005).

126 Taylor, B. S., de Vera, M. E., Ganster, R. W., Wang, Q., Shapiro, R. A., Morris, S. M., Jr., Billiar, T. R. & Geller, D. A. Multiple NF-kappaB enhancer elements regulate cytokine induction of the human inducible nitric oxide synthase gene. *J Biol Chem* **273**, 15148-15156 (1998).

127 Carta, S., Tassi, S., Pettinati, I., Delfino, L., Dinarello, C. A. & Rubartelli, A. The rate of interleukin-1beta secretion in different myeloid cells varies with the extent of redox response to Toll-like receptor triggering. *J Biol Chem* **286**, 27069-27080, doi:10.1074/jbc.M110.203398 (2011).

128 Cirstoveanu, C. G., Barascu, I. & Mc Kenzie Stancu, S. Hemadsorption with Adult CytoSorb(R) in a Low Weight Pediatric Case. *Case Rep Crit Care* **2017**, 6987167, doi:10.1155/2017/6987167 (2017).

129 Trager, K., Schutz, C., Fischer, G., Schroder, J., Skrabal, C., Liebold, A. & Reinelt, H. Cytokine Reduction in the Setting of an ARDS-Associated Inflammatory Response with Multiple Organ Failure. *Case Rep Crit Care* **2016**, 9852073, doi:10.1155/2016/9852073 (2016).

130 Trager, K., Fritzler, D., Fischer, G., Schroder, J., Skrabal, C., Liebold, A. & Reinelt, H. Treatment of post-cardiopulmonary bypass SIRS by hemoadsorption: a case series. *Int J Artif Organs* **39**, 141-146, doi:10.5301/ijao.5000492 (2016).

131 Tomescu, D. R., Olimpia Dima, S., Ungureanu, D., Popescu, M., Tulbure, D. & Popescu, I. First report of cytokine removal using CytoSorb(R) in severe noninfectious inflammatory syndrome after liver transplantation. *Int J Artif Organs* **39**, 136-140, doi:10.5301/ijao.5000489 (2016).

132 Bernardi, M. H., Rinoesl, H., Dragosits, K., Ristl, R., Hoffelner, F., Opfermann, P., Lamm, C., Preissing, F., Wiedemann, D., Hiesmayr, M. J. & Spittler, A. Effect of hemoadsorption during cardiopulmonary bypass surgery - a blinded, randomized, controlled pilot study using a novel adsorbent. *Crit Care* **20**, 96, doi:10.1186/s13054-016-1270-0 (2016).

133 Latz, E., Xiao, T. S. & Stutz, A. Activation and regulation of the inflammasomes. *Nat Rev Immunol* **13**, 397-411, doi:10.1038/nri3452 (2013).

Statutory Declaration

"I, Xiu-Ping Hu, by personally signing this document in lieu of an oath, hereby affirm that I prepared the submitted dissertation on the topic: **Signaling Pathway for Serum Amyloid A Mediating Inflammatory Reactions in Macrophages"**, independently and without the support of third parties, and that I used no other sources and aids than those stated.

All parts which are based on the publications or presentations of other authors, either in letter or in spirit, are specified as such in accordance with the citing guidelines. The sections on methodology (in particular regarding practical work, laboratory regulations, statistical processing) and results (in particular regarding figures, charts and tables) are exclusively my responsibility.

My contributions to any publications to this dissertation correspond to those stated in the below joint declaration made together with the supervisor. All publications created within the scope of the dissertation comply with the guidelines of the ICMJE (International Committee of Medical Journal Editors; www.icmje.org) on authorship. In addition, I declare that I am aware of the regulations of Charité – Universitätsmedizin Berlin on ensuring good scientific practice and that I commit to comply with these regulations.

The significance of this statutory declaration and the consequences of a false statutory declaration under criminal law (Sections 156, 161 of the German Criminal Code) are known to me."

Date Signature

Declaration of your own contribution to any publications

Results of this dissertation "Figure 9, MCP-1 detection in THP-1 macrophage after 24 h SAA and LPS stimulation", and "Figure 11 C, MCP-1 detection in THP-1 macrophage after 24 h SAA +/- antagonists" are part of a recent publication.

Xiu-Ping Hu contributed the following to the below listed publications:

Schuchardt M, Prüfer N, Tu Y, Herrmann J, Hu XP, Chebli S, Dahlke K, Zidek W, van der Giet M, Tölle M. Dysfunctional high-density lipoprotein activates toll-like receptors via serum amyloid A in vascular smooth muscle cells. Scientific Reports. 2019, doi 1038/s41598-019-39846-3

- Cell culture stimulation experiments for MCP-1 protein secretion (Figure 3 E,F)
- Analysis of results
- Read and approved the final version of the manuscript

_____

Signature, date and stamp of supervising university professor / lecturer

_____

Signature of doctoral candidate

My curriculum vitae does not appear in the electronic version of my paper for reasons of data protection.

Publications

1. Schuchardt M, Prufer N, Tu Y, Herrmann J, **Hu XP**, Chebli S, Dahlke K, Zidek W, van der Giet M, Tolle M. **2019**. Dysfunctional high-density lipoprotein activates toll-like receptors via serum amyloid A in vascular smooth muscle cells. Sci Rep 9: 3421.
2. Li Q, **Hu XP**, Sun R, Tu Y, Gong F, Ni Y. **2016**. Resolution acute respiratory distress syndrome through reversing the imbalance of Treg/Th17 by targeting the cAMP signaling pathway. *Mol Med Rep* 14: 343-8.
3. **Hu XP**, Wang RY, Wang X, Cao YH, Chen YQ, Zhao HZ, Wu JQ, Weng XH, Gao XH, Sun RH, Zhu LP. **2015**. Dectin-2 polymorphism associated with pulmonary cryptococcosis in HIV-uninfected Chinese patients. *Med Mycol* 53: 810-6.
4. **Hu XP**, Wu JQ, Zhu LP, Wang X, Xu B, Ou XT, Weng XH. **2012**. Association of Fcgamma receptor IIB polymorphism with cryptococcal meningitis in HIV-uninfected Chinese patients. *PloS one* 7: e42439.
5. Ou XT, Wu JQ, Zhu LP, Guan M, Xu B, **Hu XP**, Wang X, Weng XH. **2011**. Genotypes coding for mannose-binding lectin deficiency correlated with cryptococcal meningitis in HIV-uninfected Chinese patients. *J Infect Dis* 203: 1686-91.

Acknowledgments

Here I thank Prof. Dr. Markus van der Giet, PD. Dr. Markus Tölle and Dr. Mirjam Schuchardt for the opportunity to work in their group on this interesting project.

Furthermore, I thank Dr. Mirjam Schuchardt and PD. Dr. Markus Tölle for the help with experimental design and the evaluation of this thesis, and their other supports during my stay in this laboratory.

I thank Jaqueline Herrmann for her assistance in the cell stimulation experiments and discussion of the results.

I thank Katharina Kuschfeldt and Brigitte Egbers for their lab work assistance.

I thank Xiayun Ye for her writing correction.

Thanks to my chief Prof. Renhua Sun for the opportunity to work aboard.

Thanks to all the colleagues mentioned above, my families and friends, for their strong support during those past three years.